Seismic-induced damage in historical masonry vaults: A case-study in the 2012 Emilia earthquake-stricken area

Antonio Maria D'Altri, Giovanni Castellazzi, Stefano de Miranda, Antonio Tralli, *Seismic-induced damage in historical masonry vaults: A case-study in the 2012 Emilia earthquake-stricken area*, Journal of Building Engineering, Volume 13, 2017, Pages 224-243

ISSN 2352-7102

The final published version is available online at:
https://doi.org/10.1016/j.jobe.2017.08.005

Seismic-induced damage in historical masonry vaults: a case-study in the 2012 Emilia earthquake-stricken area

Antonio Maria D'Altri[1*], Giovanni Castellazzi[1], Stefano de Miranda[1], Antonio Tralli[2]

[1] *Department of Civil, Chemical, Environmental, and Materials Engineering (DICAM), University of Bologna, Viale del Risorgimento 2, 40136 Bologna, Italy*

[2] *Engineering Department, University of Ferrara, Via Saragat 1, 44122 Ferrara, Italy*

Abstract

The seismic analysis of historical masonry vaults is a challenging task for contemporary engineers as their behavior depends on a very huge number of factors. Among them, the vaults response is also influenced by the seismic behavior of their bearing structures. This paper aims at investigating the capabilities and limitations of current finite element-based computational tools to analyze the seismic-induced damage in masonry vaulted structures. The case under study is the Giulio II vault, located in the main tower of the San Felice sul Panaro fortress (Italy) which has been severely damaged by the 2012 Emilia earthquake. Much attention is focused on the interaction between the vault and its bearing tower. The developed finite element model includes the 3D geometry of the vault within the geometry of the tower, based on a before-quake survey. Nonlinear static and dynamic analyses are carried out by using a damage-plasticity constitutive law for masonry. Numerical results are compared to the vault actual crack pattern as well as to its actual-deformed geometry based on a post-quake laser scanner survey.

Keywords: Historical masonry vaults, Seismic damage, FE nonlinear analysis, Architectural Heritage, Laser scanner

1. Introduction

The disasters caused by past and recent earthquakes on both monumental and ordinary historical masonry buildings have induced many researchers to investigate their seismic behavior. Most of the research works were focused on studying the seismic response of vertical masonry structures [1, 2], or to analyze entire buildings also taking into account horizontal structural elements, generally constituted by timber floors or masonry vaults. In particular, these latter elements have been studied aiming at investigating their role in the seismic response of buildings. Indeed, working as horizontal diaphragms, their behavior significantly affects the overall response of the structure in terms of both strength and stiffness [3]. However, as their collapse may cause casualties and large artistic and cultural losses (e.g. the

*corresponding author: antoniomaria.daltri2@unibo.it

collapse of two frescoed vaults of the upper Basilica of St Francis of Assisi in 1997 [5]), deep investigations of their response under earthquake actions appear of primary importance. The seismic analysis of historical masonry vaults is a challenging task for contemporary engineers as their behavior depends on a very huge number of factors. Among them, the vaults response is also influenced by the seismic behavior of their bearing structures.

Another aspect which further makes challenging this topic derives from the complex geometries that characterize masonry vaulted structures. Recently, advanced surveying techniques, such as laser scanner, allow to rapidly capture the detailed geometry of complex objects. This technology has been successfully used for generating 3D models and monitoring the deformations of very complex masonry domes, see for instance [4].

Several studies have been dedicated to the analysis of masonry vaults under static vertical actions. Following [6] or [7], it can be affirmed that the modern theory of limit analysis of masonry structures, which has been developed mainly by Heyman [8, 9], is the most reliable tool to understand and analyze masonry curved structures. However, classical manual methods of analysis [7] allow to find in a suitable way 1D equilibrium solutions for the different types of vaults. The first research works on the numerical assessment of the static behavior of masonry vaults date back to the early 90s, see for instance the pioneering studies on the Brunelleschi Dome in [10]. As regards recently developed computational methods we can classify them into two broad categories [11]: (i) Thrust network methods, based on the Static Theorem of the limit analysis [12]-[16], and (ii) Finite and Discrete Element Methods, developed both for limit analysis and for nonlinear incremental analysis (see for instance FEM approaches in [17]-[24] and DEM approaches in [25]-[27]).

Concerning the studies published since 2000 it is possible to observe that a number of commercial software packages have been often used in the scientific literature to model masonry vaults. These programs are mostly FE codes developed to study concrete structures employing complex plastic-damaging constitutive models: cracks are taken into account as a kind of smeared distortions. The heterogeneity of masonry is not accounted for and isotropic behavior either in the elastic field or at collapse is generally assumed. However, it is worth noting that these techniques of analysis turn out to be adequate if combined with proper engineering reasoning. However, there is still much work to do on the definition of constitutive equations for masonry in the dynamic field. For example, with no claim to be exhaustive, the authors mention that: DIANA TNO [23] and NOSA CNUCE [24] contain specific software developed for studying masonry shells; [17] used ANSYS by assuming for masonry elastic-plastic material models (either Drucker-Prager or Willam-Wranke with low tension strength); [15] used Algor V21 with contact elements; [21] employed Abaqus by adopting a damage-plasticity approach.

However, only few of the cited papers are specifically addressed to the seismic analysis of masonry vaults. Moreover, they seem efficient for laboratory samples only, while the seismic behavior of historical masonry vaults strictly relies on the seismic response of the bearing structure. Accordingly, the numerical modeling of a historical masonry vault under earthquake actions cannot disregard the modeling of the bearing structure. Despite the problem importance, the role played by the structure on which the vaults rest has not been thoroughly studied.

With this in mind, this paper investigates the capabilities and limitations of current computational tools to simulate the seismic-induced damage in complex masonry vaulted structures. The case under study is the Giulio II vault, located in the main tower of the San Felice sul Panaro fortress (Italy) which has been severely damaged by the 2012 Emilia earthquake. The San Felice sul Panaro fortress has been subjected to several recent scientific studies. In particular, advanced FE mesh generation approaches have been proposed and applied to the fortress in [28, 29, 30, 31, 32]. Additionally, thorough numerical investigations on the seismic behavior of the main tower of the fortress have been carried out and some of the results are collected in [33, 34]. Particularly, the influence of adjacent buildings on the dynamic behavior of the main tower have been inspected in [34] where, in order to limit the computational effort, masonry vaults and timber floors have been modeled through equivalent plates (i.e. with the same in-plane stiffness), according to [3].

Here, the attention is focused on the modeling and analysis of the Giulio II vault and, particularly, on the interaction between the vault and its bearing system. The developed finite element model includes the 3D geometry of the vault within the geometry of the tower, based on a before-quake survey. Nonlinear static and dynamic analyses are carried out by using a damage-plasticity constitutive law. The results are compared to the vault actual crack pattern as well as to its actual-deformed geometry, based on a post-quake laser scanner survey.

The paper is organized as follows. Section 2 presents the case study, Section 3 illustrates the numerical modeling of the vault and Section 4 presents and discusses the numerical results, obtained by both nonlinear static and dynamic analyses. Concluding remarks end the paper (Section 5).

2. Description of the case study

The masonry vault which covers the Giulio II Hall in the main tower of the San Felice sul Panaro fortress (Figure 1), a town located near the city of Modena (Italy), is investigated. Such a cross vault (Figure 2) is located between the II and the III level of the main tower of the fortress (the tower on the right of Figure 1) and is characterized by an almost squared plan of approximately 6.5 meters, small ribs and a fresco (which portraits Saint Francis of Assisi) on its North side (Figure 2(c)). This latter artistic element further increases the heritage value of the case study, as commonly occurs for historical buildings [35, 36].

2.1. Historical notes

The San Felice sul Panaro fortress exhibits a very complex historical evolution along the centuries which also characterizes the Giulio II Hall's vault. Indeed, from the construction, which started in the XIV century, several alterations, modifications and reshuffles have taken place depending on the intended use changes of the parts of the monument. Consequently, the drafting of a very precise and accurate historical reconstruction of the evolution phases of the fortress, and in particular of the studied vault, was substantially impossible due to several lacks in the historical documents.

Figure 1: San Felice sul Panaro fortress.

Among the interesting documented events, it is worth noting that in 1511, when San Felice sul Panaro town was involved in conflicts between the Houses of Pico, Pio and Este, Pope Jiulius II (Giulio II in Italian) sojourned in the fortress and still nowadays there is a room which bears his name (the Giulio II Hall). Indeed, for such an occasion a vaulted room in the main tower of the fortress was prepared and two openings in the room, one as a door (in the North side) and the other as a window (in the South side), were realized by demolishing portions of the walls. Successively, one of the two aforementioned openings was closed.

Another relevant event which characterize the (more recent) history of the main tower (and consequently of the Giulio II Hall's vault) consists of the construction, in 1920, of a heavy cylindrical water reservoir made out of reinforced concrete in the IV level of the tower. The cracking pattern appeared immediately after the first replenishment of the tank (which principally consists in a sub-vertical crack from the V to the III level in the North side) forced the emptying and later the complete dismantlement of the tank and the closing of the cracks.

Among the more recent intended use of the Giulio II Hall, in 1999 the room was set up for an archaeological exhibit as depicted in Figure 2(a) and Figure 2(b). In 2012 the fortress, and consequently the Giulio II Hall's vault, was severely damaged by the Emilia earthquake. The last arrangement of the Giulio II Hall before the earthquake is reported in Figure 2(c). More details are reported in the following.

2.2. Emilia earthquake damage

During the second half of May 2012, the Emilia-Romagna region experienced a strong seismic sequence which particularly damaged the historical architectural heritage of the area [37, 38, 39]. In particular, the biggest quakes occurred within the provinces of Modena and Ferrara. The main shocks have been recorded on May the 20th ($M_w = 5.9$) and May

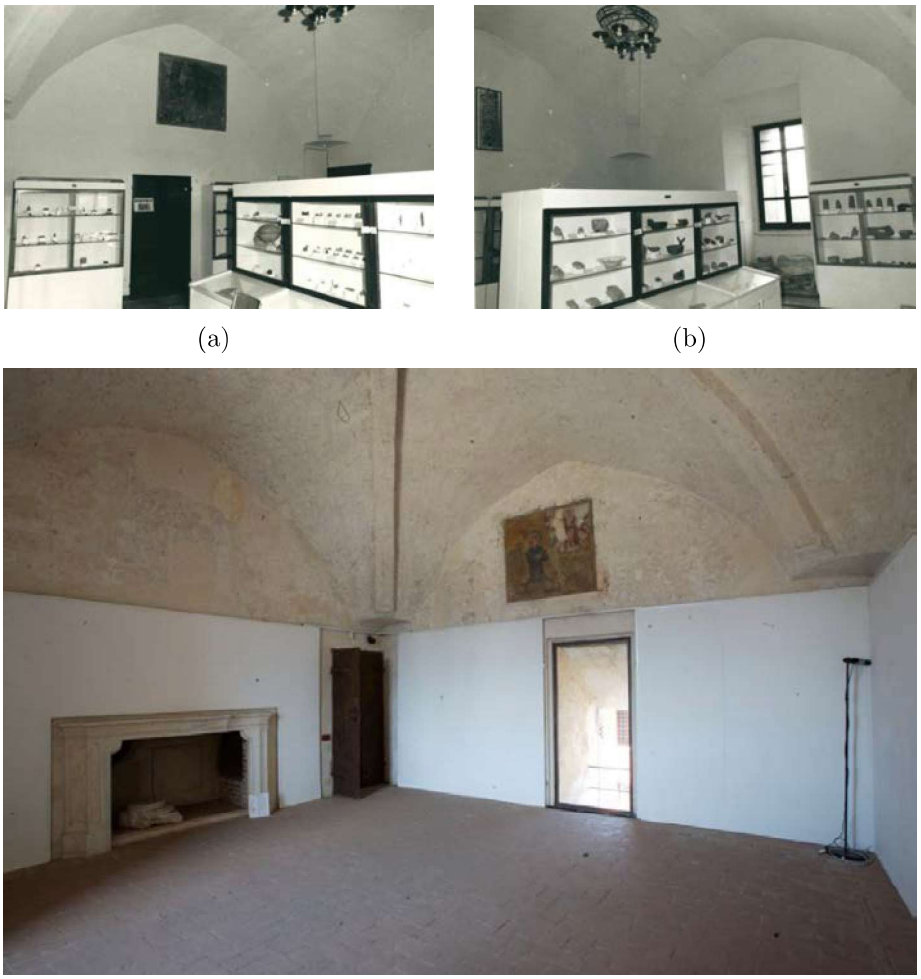

(a) (b)

(c)

Figure 2: Giulio II Hall before the Emilia Earthquake.

the 29th ($M_w = 5.8$) [40, 41], whose epicenters have been located at about 10 and 5 km from San Felice sul Panaro, respectively [42]. An accurate outline of the damage experienced by Emilian medieval fortresses due to the seismic sequence is reported in [43].

As a result, the fortress presented a widespread damage characterized by the collapse of the crowning of the minor towers and the appearance of several deep cracks on the main tower. In particular, the most relevant cracks appeared on the main tower consisted in diagonal cracks, clearly visible in the lower half of the South (Figure 3(a)) and North (Figure 3(b)) front. Approximately, these two main cracks are placed in the same plane, roughly perpendicular to the line individuated by points H and L in Figure 3(c).

In the Giulio II Hall (whose position is highlighted by red frames in Figures 3(a) and 3(b) and by a blue dotted frame in Figure 3(c)), the vault which cover the room has been interested by the presence of deep cracks and partial collapses, see Figures 4 and 5. In general, it can be noted that the big flue chimney which is present inside the West wall of

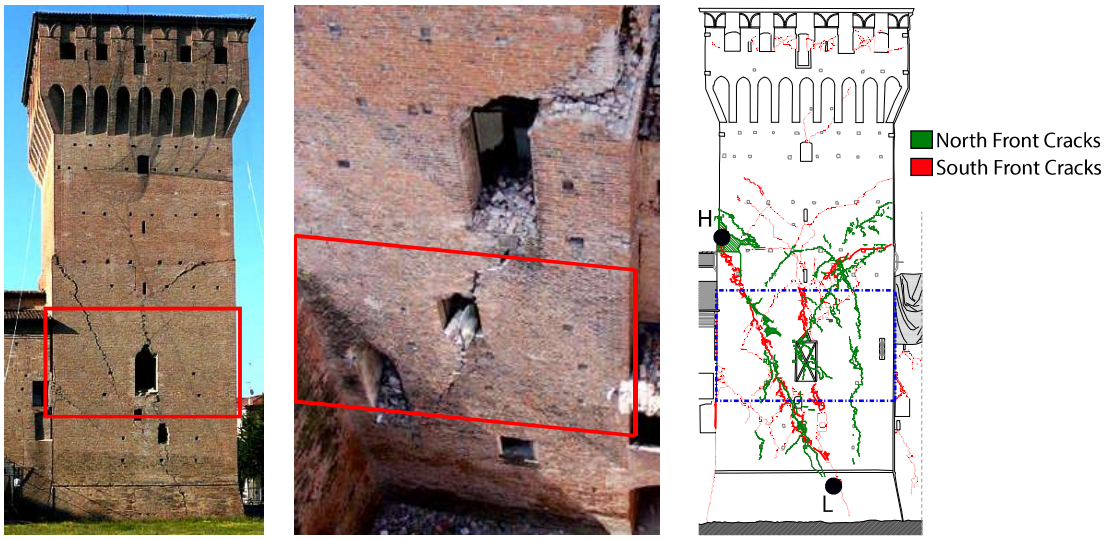

(a) (b) (c)

Figure 3: Main tower of San Felice sul Panaro fortress after the Emilia earthquake (2012): (a) Main tower's South front, (b) North front and (c) South and North fronts cracks superposition.

the tower could have weakened the masonry structure [43]. More specifically, by inspecting Figure 4, the presence of four major failures of the vault, which are highlighted by the letters a, b, c and d and are magnified in Figure 5, can be noted. In particular, by inspecting the vault intrados the more severe damages can be summarized as follows:

(a) a collapse of a part of the vault near the flue chimney (West side), see Figure 5(a);

(b) a main and very severe crack which substantially cut in two parts the Giulio II Hall, highlighted by blue arrows in Figure 4, see details in Figure 5(b);

(c) the detachment and collapse of the ribs, see Figure 5(c);

(d) a deep crack which starts from the upper extremity of the South-side-window, passes near the vault's keystone and ends in the opposite side, see Figure 5(d).

The aforementioned damage pattern could be plausibly explained as follows:

- the partial collapse (a) could be due to the presence in previous times of an opening in the vault for a stairwell inside the tower. Successively, due to the change of the tower's intended use from defense purposes to residence the stair could have been removed and the vault could have been closed. However, a discontinuity between the reshuffled part and the original one due to a non-optimal toothing could have represented a weakness zone during the seismic excitation leading to a local collapse. Moreover, the aforementioned presence of the chimney hole in the West side could have weakened the purpose of the bearing structure in such vault portion;

- the main crack (b) which passes through the vault along the N-S direction substantially links the two major diagonal cracks experienced by the main tower's South side (Figure 3(a)) and North side (Figure 3(b)), as also shown in Figure 3(c);

- the detachment and collapse of the ribs (c) could be due to the fact that in this case the vault's ribs were added after the vault's construction. The role of the ribs in the mechanical behavior of masonry cross vaults has been the subject of intense debates since the 19th century [9, 44] and numerical analyses have been employed to investigate their effects [45]. However, the hypothesis of later decorative non-structural ribs is made by the authors due to the presence of an almost regular layer of a relatively recent cementitious mortar between the ribs and the vault (Figure 5(c)).

- the crack (d) starts from the window in the South side of the tower (Figure 5(d)). Such an opening was obtained by demolishing a portion of the wall, as said before. This fact, as well as the absence of an adequate lintel over the opening, could have weakened this part of the structure.

Summing up, it emerges that the damages experienced by the vaulted structure during the earthquake are strictly linked to its historical evolution phases (e.g. failures (a), (c) and (d) in Figures 4 and 5) and to the seismic-induced damage experienced by the masonry tower, i.e. the vault's bearing structure (e.g. failure (b) in Figures 4 and 5).

Finally, it has also to be pointed out that the perimeter wall of the East side of the Giulio II Hall detached from the floor of approximately 6 centimeters (Figure 6), while in the other sides no relevant detachments appeared.

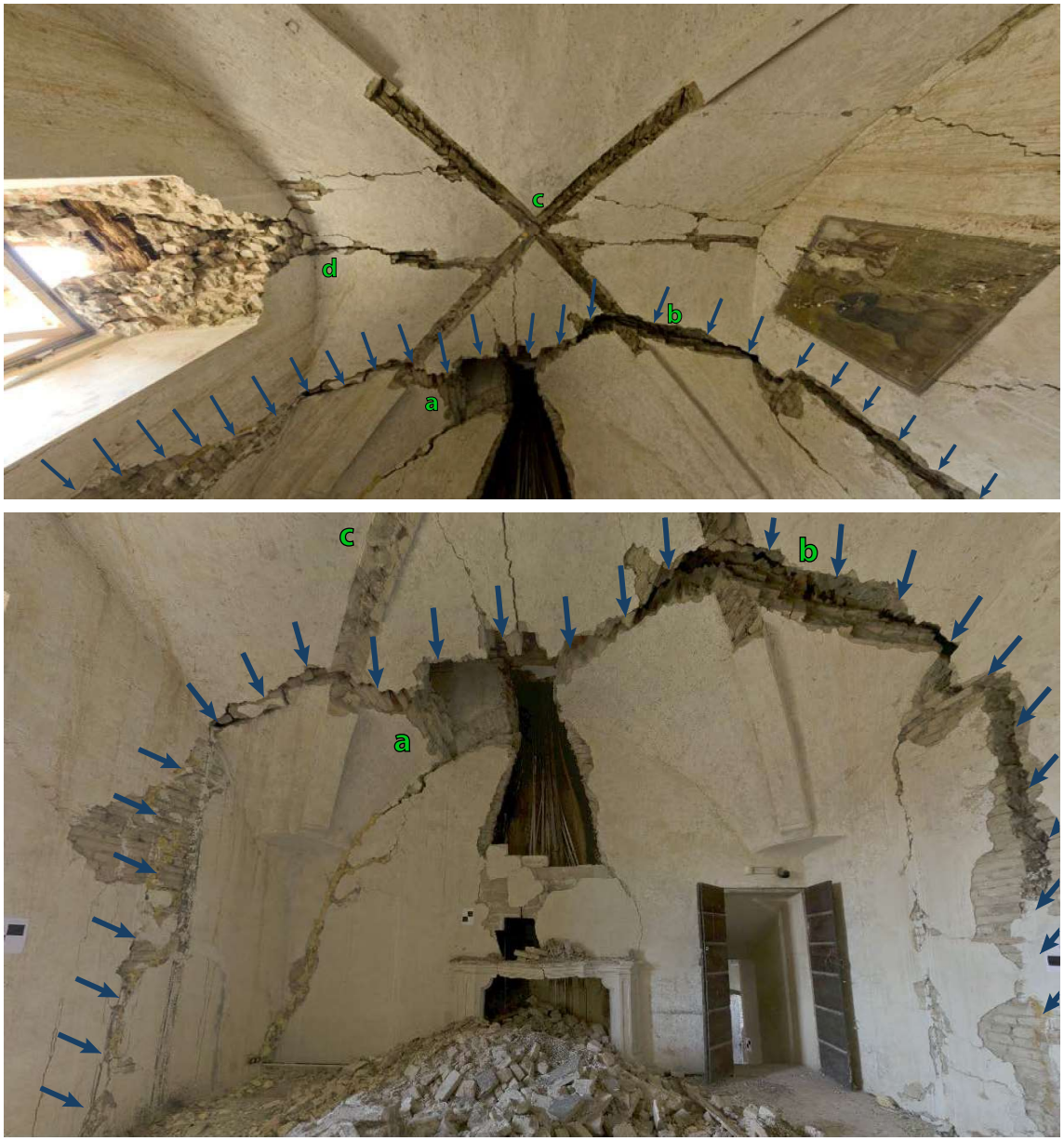

Figure 4: Giulio II Hall's vault after the Emilia earthquake.

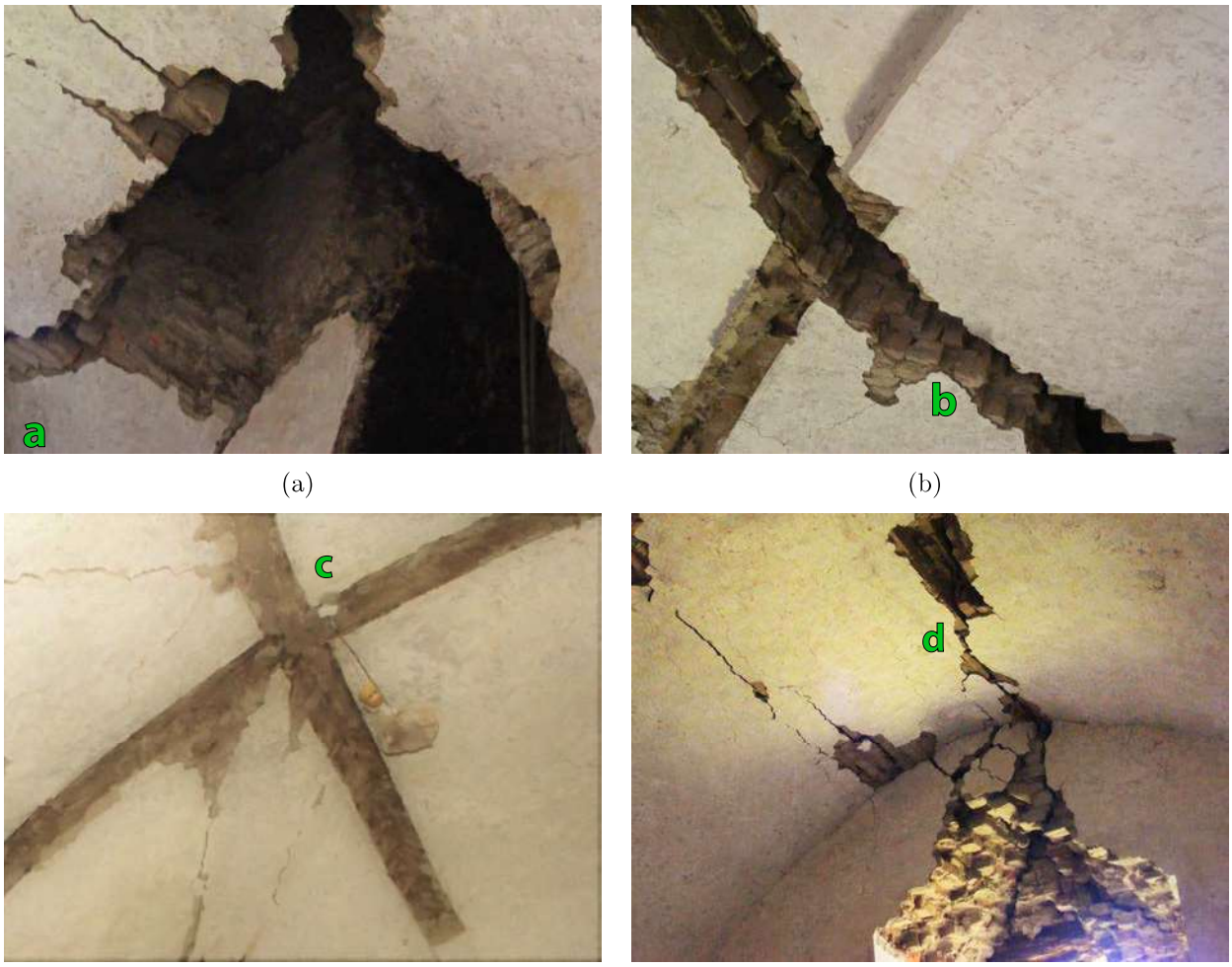

(a) (b)

(c) (d)

Figure 5: Giulio II Hall's vault major failures. The letters a, b, c and d are referred to Figure 4.

Figure 6: Detachment between the floor and the East wall of the Giulio II Hall after the Emilia earthquake.

2.3. Vault surveys

Aiming at quantitatively assessing the effects of the seismic action on the vault, a comparison between two different surveys, one made in 1985 (the only available before the earthquake) and one made in 2012 after the earthquake, has been carried out in terms of vault's abutments relative displacements. However, it has to be pointed out that the two geometrical surveys were conducted in different times with completely different techniques characterized by different accuracy. In particular, the first one was performed in 1985 with classical hand-based survey procedure, whereas the second one was carried out in 2012 with the laser scanner technique. Coarsely, if the first one guarantees the accuracy of some centimeters, the second one guarantees the accuracy of some millimeters. The comparison of the Giulio II Hall's vault plan before and after the seismic event is reported in Figure 7, while the comparison of its N-S section and its E-W section is reported in Figure 8. Concerning Figure 7, it should be noted that it is not precisely know at what height the plan of Figure 7(a) (1985 survey) is taken (there is about 1 m of uncertainty).

The resulting actual relative displacements of the vault's abutments measured between the plan of Figure 7(a) and the plan of Figure 7(b) are collected in Table 1. The letters O, A, B and C are referred to Figure 7(b). As can be noticed in Table 1, relevant relative displacements have been recorded: the two diagonals of the vault (OB and CA) measure an increase of length of more than 14 cm; the sides along the E-W direction measure an increase of length of 13 cm (OA and BC) whereas the sides along the N-S direction presented shorter relative displacements of 7 (CO side) and 2 cm (AB side). Due to the different nature of the two compared surveys, the quantities collected in Table 1 have to be considered as affected by some uncertainties of the order of magnitude of centimeters. No other experimental findings are available for the Giulio II Hall's vault (in terms, for instance, of endoscope tests) since its compromised safety condition did not permit any experimental test. Therefore, no detailed information of the stratigraphy of the vault are available. However, by visually inspecting the vault's deep cracks, the assumption of 42 cm thickness has been made.

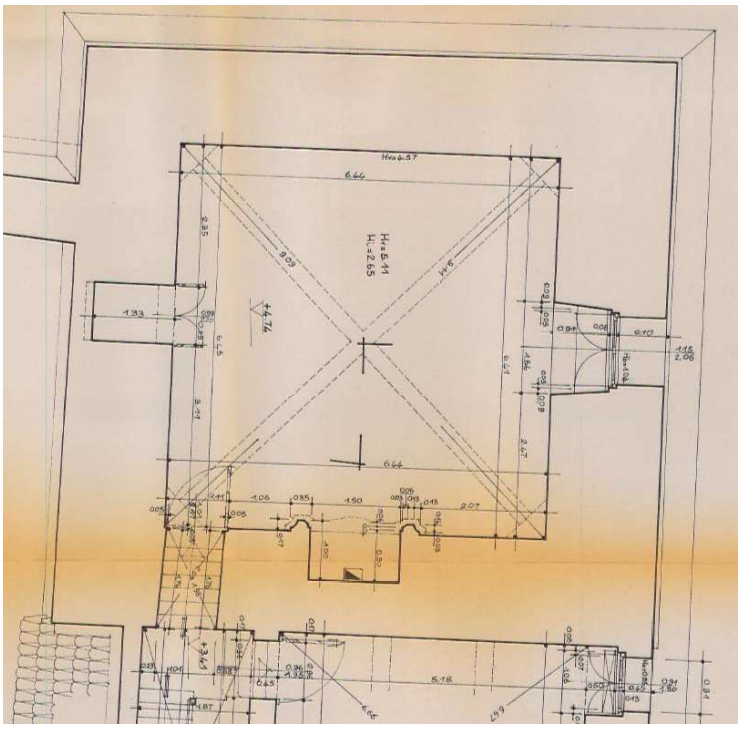

(a)

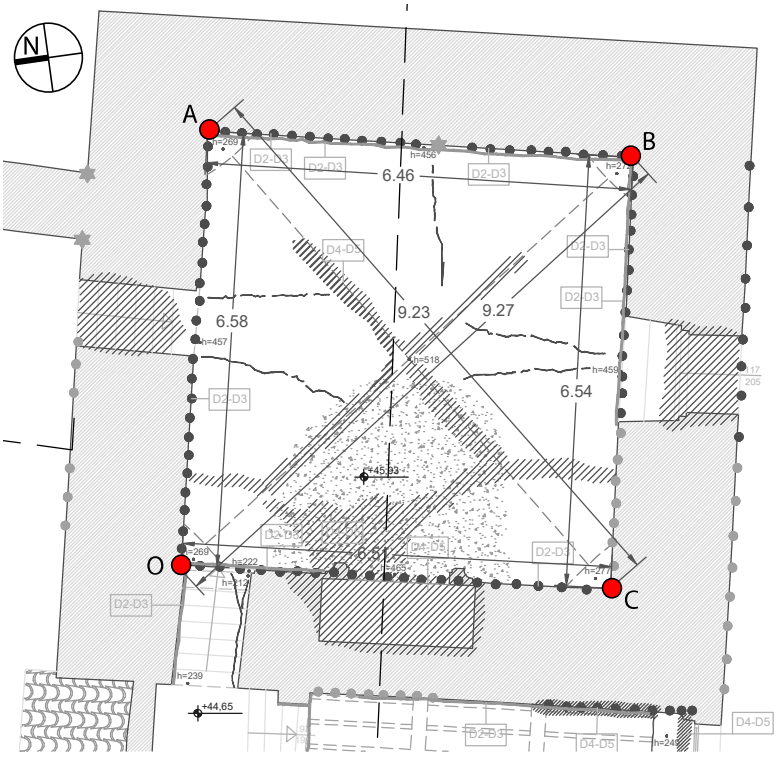

(b)

Figure 7: Giulio II Hall's vault plan: (a) before the earthquake (1985 survey) and (b) after the earthquake (2012 laser scanner survey).

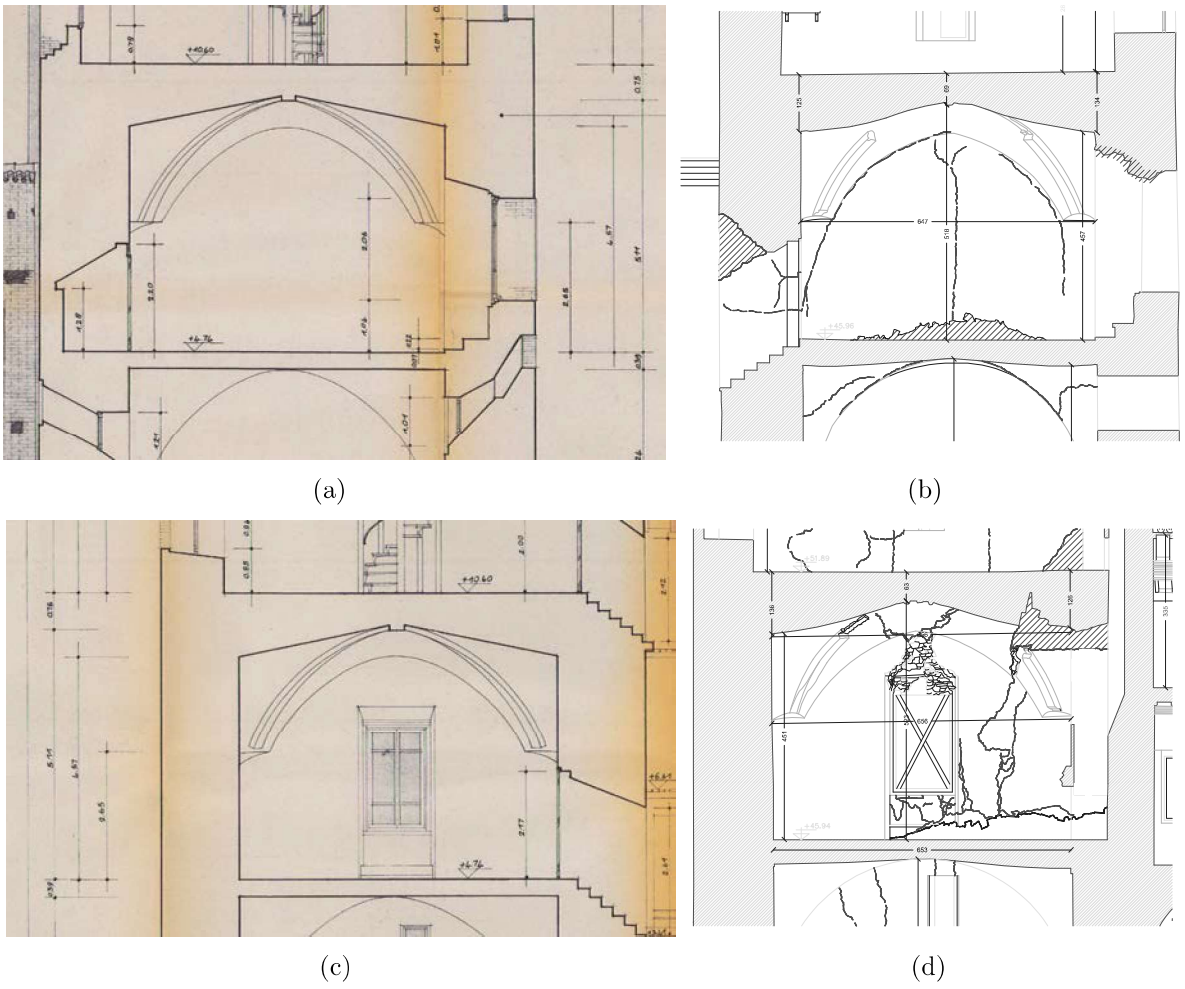

Figure 8: Giulio II Hall's vault sections: N-S section (a) before (1985 survey) and (b) after the earthquake (2012 laser scanner survey), E-W section (c) before and (d) after the earthquake.

Table 1: Relative displacements of the vault's abutments according to the measurements made before and after the earthquake, see Figure 7.

Vault's side	1985 survey	2012 survey	Rel. displ.
OA	645 cm	658 cm	13 cm
AB	644 cm	646 cm	2 cm
BC	641 cm	654 cm	13 cm
CO	644 cm	651 cm	7 cm
OB	911 cm	927 cm	16 cm
CA	909 cm	923 cm	14 cm

3. Numerical modeling

The numerical modeling of the case-study has been carried out through a 3D FE model. The geometry has been obtained through a 3D CAD modeling, based on the 1985's survey (before earthquake). As anticipated, the vault 3D FE model is included within the 3D FE model of the tower having, hence, a unique detailed model. This choice is crucial in order to investigate how the seismic behavior of the tower influences the seismic-induced damage of secondary elements such as vaults, given their mutual and direct interaction.

Based on the vault's survey, the following assumptions in the numerical modeling of the vault are made:
(i) absence of ribs, since they appear to have only a decorative function, see Figure 5(c);
(ii) vault without any hole, to model the vault condition before the earthquake;
(iii) equivalent masses have been applied on the vault in order to take into account the infill weight, made up of a heterogeneous material, and the pavement.

The 3D FE mesh of the tower, which includes the vault, is depicted in Figure 9. Horizontal axes of the model (X and Y) substantially correspond to the cardinal directions (S-N and E-W, respectively). In order to maintain acceptable the computational cost, the mesh design aimed at guaranteeing a fine description of the vault and a coarser description of the tower. In any case, the presence of at least three tetrahedron elements on the thickness of the tower trunk's walls (Figure 9(c)) guarantees a reasonable accuracy in terms of global structural behavior of the tower. The adopted FE mesh counts 20,393 nodes and 79,459 tetrahedron elements.

As extensively discussed in [34], the seismic behavior of the tower is influenced by the presence of adjacent structural elements. Therefore, some portions of the adjacent buildings have been considered in the FE model (Figure 9(a)). Therefore, in order to approximately take into consideration the stiffness of the non-meshed parts of the fortress while keeping simple the model and low the computational effort, rollers have been inserted on the surfaces highlighted by purple arrows, see Figure 9(a).

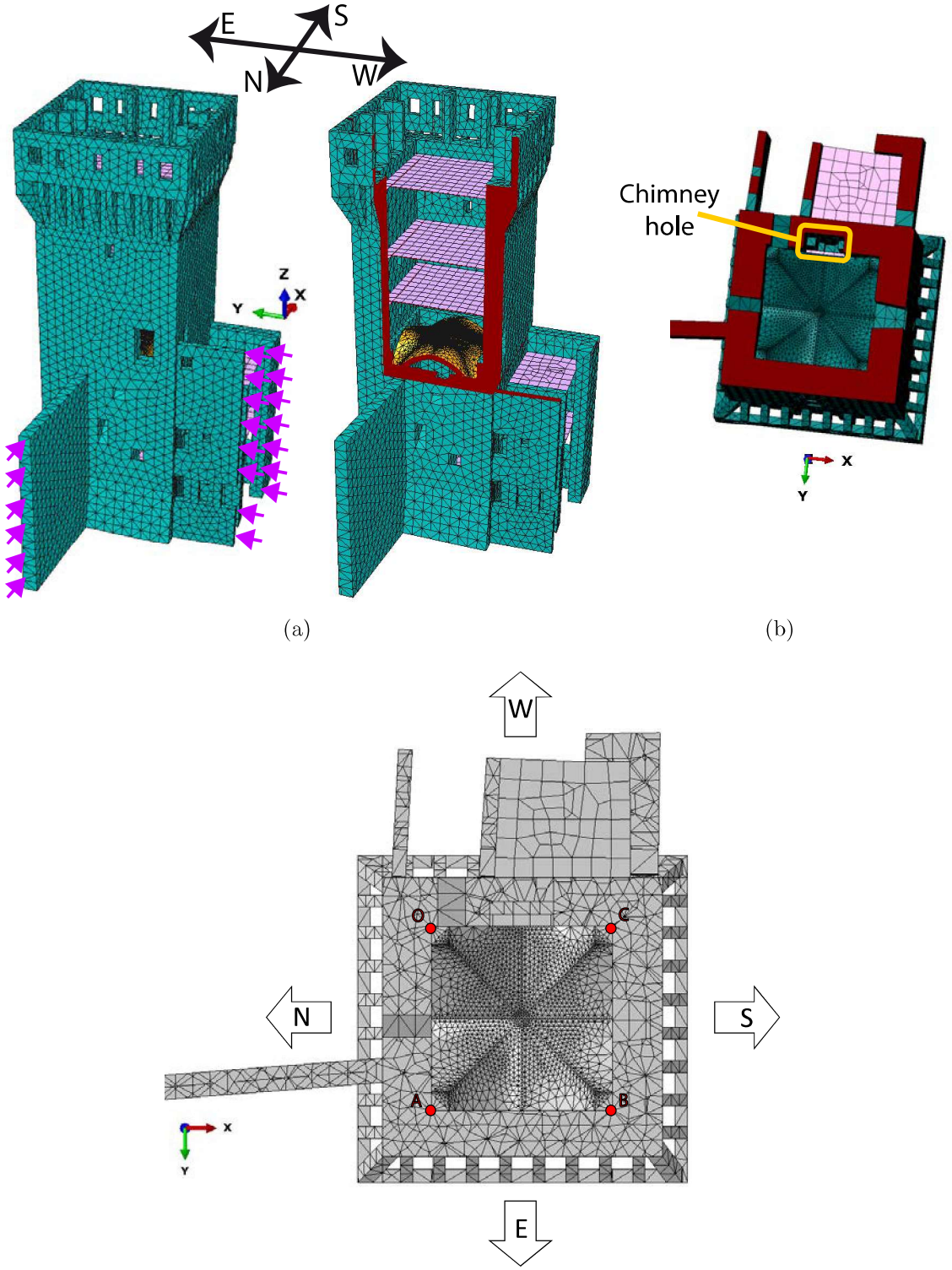

Figure 9: Vault and the tower's 3D FE numerical modeling: (a) 3D FE mesh, (b) particular of the chimney hole and (c) Giulio II Hall's vault mesh with the considered points of the model, bottom view.

3.1. Constitutive model for masonry

The implementation of constitutive models able to simulate the mechanical behavior of masonry is a challenging task, especially in dynamic simulations. Masonry is characterized by an orthotropic behavior, both in the linear and nonlinear fields [46]. Interesting progresses have been achieved in masonry orthotropic damage models [47], even if their application to 3D large-scale problems appears inefficient due to their high computational demand and, hence, their limitation to small-scale structures. For this reason, the use of isotropic damage models for full-scale masonry structures is commonly accepted [29]. In particular, the case study presents very thick walls with a chaotic masonry texture, for which a orthotropic model appears as questionable as an isotropic one.

In this paper, isotropic material behavior has been assumed and the Concrete Damage Plasticity (CDP) model, available within the Abaqus software [48], has been used to perform nonlinear static and dynamic analyses. Even though such a model has been designed for concrete, the authors experienced successful results for masonry structures, see for instance [29, 34]. The material properties as well as the model parameters used in numerical analyses are collected in Table 2. In the following, the main model parameters are briefly discussed. The interested reader is referred to [48, 29] for more details.

Table 2: Material properties and model parameters used in numerical analyses.

Material properties and parameters		Values	
Young's modulus E_0 $[MPa]$		1500	
Poisson's ratio		0.2	
Dilatation angle		10	
Eccentricity		0.1	
f_{b0}/f_{c0}		1.16	
K_c		2/3	
Viscosity Parameter		0.002	
Tensile mono-axial curve		Compression mono-axial curve	
Stress $[MPa]$	Inelastic strain	Stress $[MPa]$	Inelastic strain
0.12	0	2.0	0
0.0012	0.001	2.4	0.002
0.0012	0.003	0.2	0.007

The CDP model uses a Drucker-Prager strength criterion, modified through a parameter, K_c, which represents the ratio between the distance from the hydrostatic axis of the maximum compression and tensile stress [48, 49, 50]. Furthermore, the CDP model considers an eccentricity parameter, which serves to regularize the tensile corner, and a nonassociated potential flow rule for the elasto-plastic deformation part. Such a feature gives the possibility to account for the dilatance phenomenon, governed by the dilatation angle, which has been assumed equal to 10 degrees [51, 52]. The ratio between the bi-axial, f_{b0}, and mono-axial, f_{c0}, compression strength has been supposed according to [46]. In order to better ensure the algorithm convergence in the nonlinear range, viscoplastic regularization is implemented and

is defined through a viscosity parameter, assumed in agreement with the outcomes emerged in [29].

The damage effects consist in the gradually reduction of the Young's modulus every time the strain reaches a critical value. The following standard relationships define the mono-axial tensile σ_t and compressive σ_c stresses:

$$\sigma_t = (1 - d_t)E_0(\varepsilon_t - \varepsilon_t^{pl})$$

$$\sigma_c = (1 - d_c)E_0(\varepsilon_c - \varepsilon_c^{pl})$$

where E_0 is the initial elastic modulus, d_t and d_c are the scalar damage variables in tension and in compression, ε_t and ε_c are the total strain in tension and in compression, ε_t^{pl} and ε_c^{pl} are the equivalent plastic strain in tension and in compression. In addition, such a constitutive model accounts for the effect of closing of previously formed cracks under dynamic loading conditions, which results in the recovery of the compression stiffness.

The choice of mechanical properties for historical masonry is a challenging task. The availability of extensive destructive and non-destructive in situ tests should help the analyst in calibrating the mechanical model. However, such tests are generally expensive and invasive. Furthermore, their reliability for historical buildings is reduced due to the irregularities which characterize such structures.

No comprehensive results of experimental tests were available for the case study and, aiming at defining the material mechanical properties, it was essential to refer to national codes for existing buildings [54, 55, 56]. Material properties have been assumed considering the lowest level of knowledge (the so-called LC1 in [54]) and a clay bricks masonry with very poor mortar and quite regular texture. In addition, tensile and compression mono-axial curves (see Table 2) have been implemented according to [53], where the numerical investigations of two coeval case studies of similar masonry towers, located approximately at 10 km far from the case study under consideration, have been presented. Indeed, it is worthy to point out that medieval buildings in the area stricken by the 2012 seismic sequence exhibited a quite similar masonry strength [57]. Finally, a linear reduction until 90% of the Young's modulus with respect to E_0 for an inelastic deformation equal to the lower extremity of compressive and tensile softening branches (Table 2) has been assumed.

4. Numerical analyses

In order to investigate the seismic-induced damage in the considered historical cross vault, nonlinear static and dynamic analyses are performed on the 3D FE model depicted in Figure 9. The analyses are especially focused on the mutual interaction between the tower and the vault and, hence, particular attention is devoted to the vault abutments displacements. Figure 9(c) shows the considered points of the vault abutments used to compute displacements in the following analyses.

4.1. Nonlinear static analyses

Nonlinear static analyses have been performed by applying along the tower's principal axes horizontal forces derived by the assumption of a linear variation of acceleration along the height (called G1 in [54]). This distribution is, generally, the most critical for such kind of structures [52]. Such analyses are pushed over a drop of 20% of the base shear of the tower.

Figures 10, 11, 12 and 13 illustrate the base shear-vault abutments displacements curves for the East, West, South and North load cases, respectively. On one hand, in the East (Figure 10) and South (Figure 12) load cases the vault's abutments tend to significantly distance themselves. In particular, points belonging to the side which is pushed outwards (i.e. A and B for the East load case and B and C for the South load case) show larger displacement than the others of the same load case. Furthermore, points belonging to the same side perpendicular to the force direction record similar displacement in this two load cases. On the other hand, the West load case (Figure 11) shows a quasi-linear behavior and, also after the failure of the tower, the relative displacements of the abutments are considerably lower than the other load cases. As can be particularly noted in Figure 11, the displacements at null base shear are different from zero. This is due the fact that before pushing the structure horizontally, the model is subjected to a vertical gravitational load which produces slight horizontal displacements of the vault abutments. Finally, concerning the North load case (Figure 13), it appears that Point O's displacement is clearly larger than Point A's one, although they belong to the same side perpendicular to the horizontal force, highlighting a torsion of the tower. This phenomenon could be addressed to the presence of the curtain wall in the North side, as further discussed in the following.

Summing up the results, Figure 14 illustrates the base shear-relative displacements curves between the points which belong to vault sides parallel to the applied force. It is worth-noting that for the East directed force the abutments tend to distance themselves for base shear values slightly lower than the other cases. In addition, both the load cases East and South show similar relative displacement between the two sides parallel to the applied force for each analysis (i.e. between AO and BC and between CO and BA). In particular, in the East load case the side AO gains distance earlier than side BC, plausibly due to the fact that the North side of the tower presents three almost aligned openings (see Figure 9) which reduce the capacity of the structure's side. Furthermore, concerning the North load case it can be noted that, as already mentioned before, the side OC records relative displacement considerably greater than the other side AB. This effect could be reasonably addressed to the presence of the curtain wall in the North side of the tower (see Figure 9(a)) which acts as a North directed displacement constraint and limits the abutment A displacements. Finally, in the West load case the effect of the constraint offered by the tower's adjacent building in the West side (Figure 1) is essential and consists in a substantial limitation of the absolute displacement of the vault abutments. In particular, such a constraint almost exactly acts until the height of the vault abutments, see Figure 9. Consequently, the abutments' displacements are considerably limited (Figure 11). Moreover, the constraint offered by the adjacent building is overall uniform and no significant torsion of the tower is recorded, see Figure 14.

Table 3 collects the relative displacements of the vault's abutments at the ultimate displacement of the tower, i.e. when the base shear shows a drop of 20%. Such displacements are also highlighted on the curves of Figure 14 through a hexagon. As can be noted, the East and South load cases show greater relative displacements at the ultimate condition than the other load cases (included between 5.8 and 7.4 cm). This fact could also be addressed to the presence of adjacent structural elements in the other directions.

In Figures 15, 16, 17 and 18, damage contour plots of the four load cases (East, West, South and North, respectively) are reported for three subsequent simulation instants. In particular, in order to compare the evolution of the damage for each analysis these plots have been taken (a) at a step right after leaving the linear regime, (b) at an intermediate step between the first instant and the ultimate condition and (c) at the ultimate condition of the tower.

Concerning the East load case, the damage contour plots (Figure 15) show the development of a crack in the intrados which is perpendicular to the East direction. In particular, the development of this crack is already clear at the first considered instant, see Figure 15(a). In addition, such a crack is in good agreement with the actual crack pattern experienced by the vault, for instance compare Figure 15(b) with Figure 4 (failure (b)). Furthermore, from the second instant on out it appears a crack perpendicular to the East direction also in the vault extrados, see the section view of Figures 15(b) and 15(c). Although no reference is available for the vault extrados actual crack pattern, by inspecting Figure 6 it clearly appears that the main crack (b) crosses the whole thickness of the vault.

As far as the West directed force analysis is concerned, the strong interaction with the adjacent building, which deeply limits the structure displacements along the West direction, restricts the damage in the higher part of the tower's trunk and no significant cracks appear in the vault (Figure 16).

For what concern the South load case, as already noted in Figure 14, the points of the sides parallel to the force direction tend to distance themselves in a similar way. This is also confirmed by the damage contour plots of Figure 17 which show the progressive development of a crack in the intrados perpendicular to the South direction.

Concerning the North load case, due to the strong interaction with the curtain wall, the torsion of the tower is recorded (as reported in Figure 14) and the damage pattern of the vault (Figure 18) is conditioned by this effect. Indeed, in the vault intrados it emerges a crack which approximately tends to link the contact point with the curtain wall and the point C (Figure 9(c)) of the vault, see the progression of such a crack in Figure 18. This crack is in agreement with the actual crack specular to the failure (d) in Figure 4.

Summing up, nonlinear static analyses seem to be qualitatively able to investigate the main weaknesses of the vault.

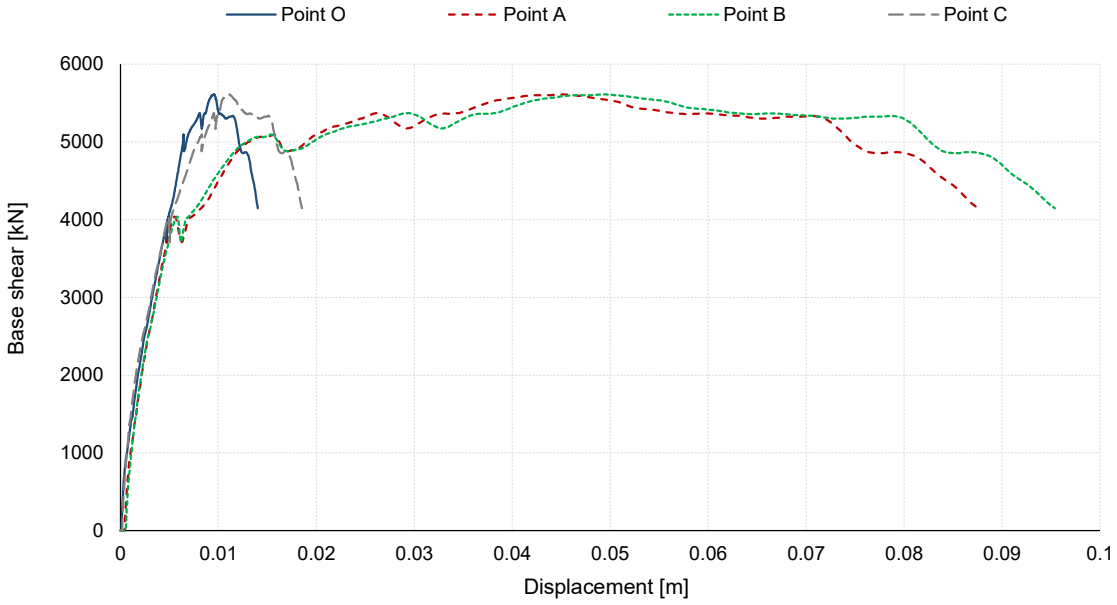

Figure 10: Base shear-displacement of the vault's abutments curve of the points depicted in Figure 9(c), East directed force.

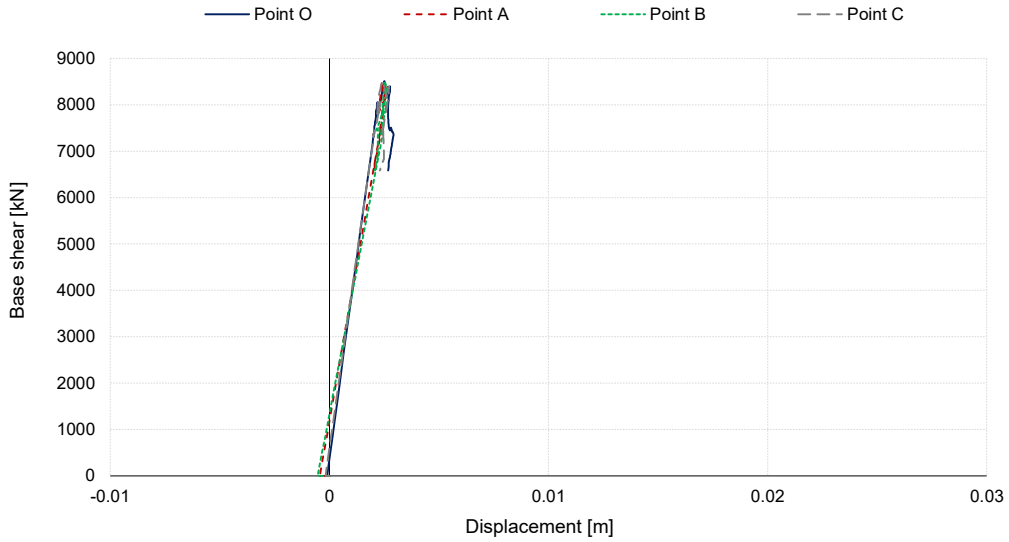

Figure 11: Base shear-displacement of the vault's abutments curve of the points depicted in Figure 9(c), West directed force.

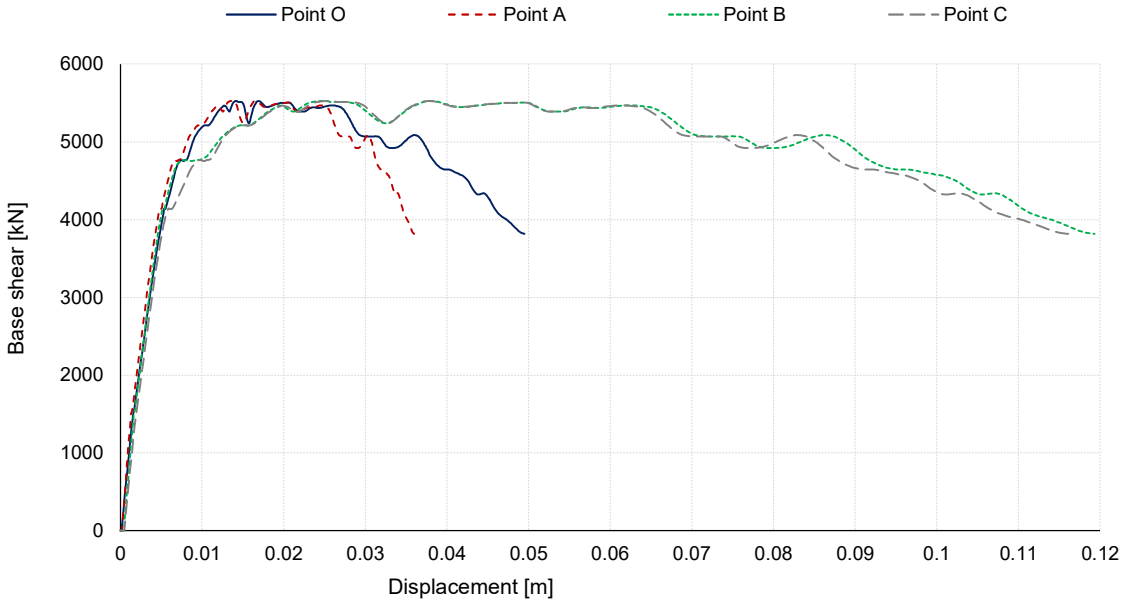

Figure 12: Base shear-displacement of the vault's abutments curve of the points depicted in Figure 9(c), South directed force.

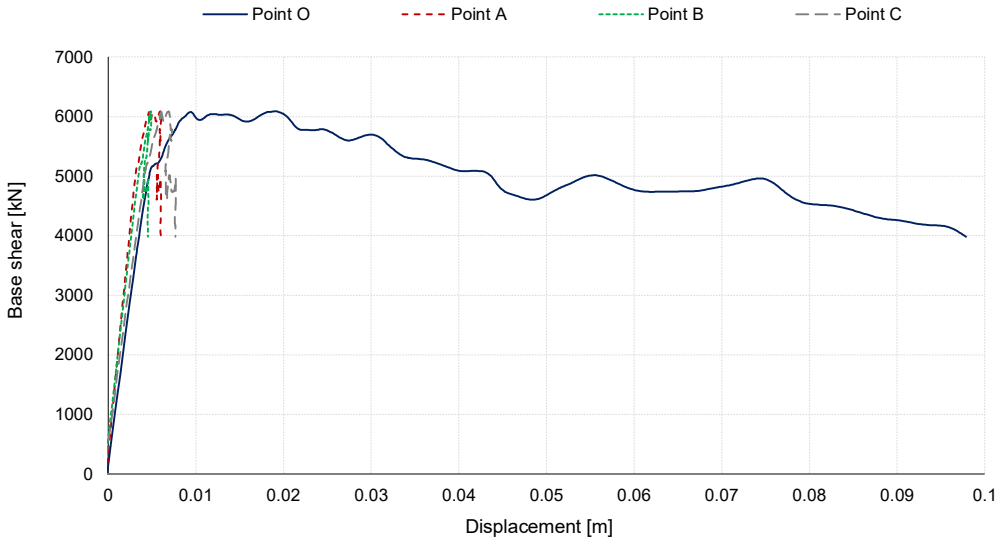

Figure 13: Base shear-displacement of the vault's abutments curve of the points depicted in Figure 9(c), North directed force.

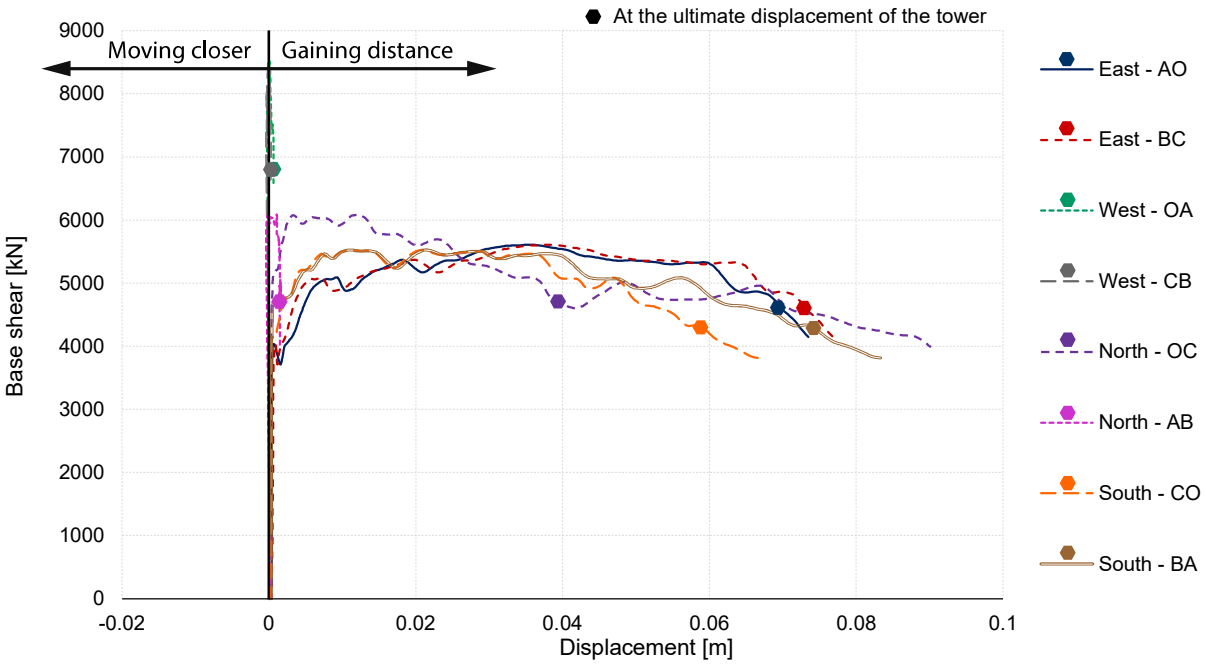

Figure 14: Base shear-relative displacement of the vault's abutments curves between the points depicted in Figure 9(c).

Table 3: Relative displacements of the vault's abutments at the ultimate displacement of the tower.

Direction	Side	Relative displacement
E	ΔAO	6.9 cm
E	ΔBC	7.3 cm
W	ΔOA	0.1 cm
W	ΔCB	0.1 cm
N	ΔOC	3.9 cm
N	ΔAB	0.2 cm
S	ΔCO	5.8 cm
S	ΔBA	7.4 cm

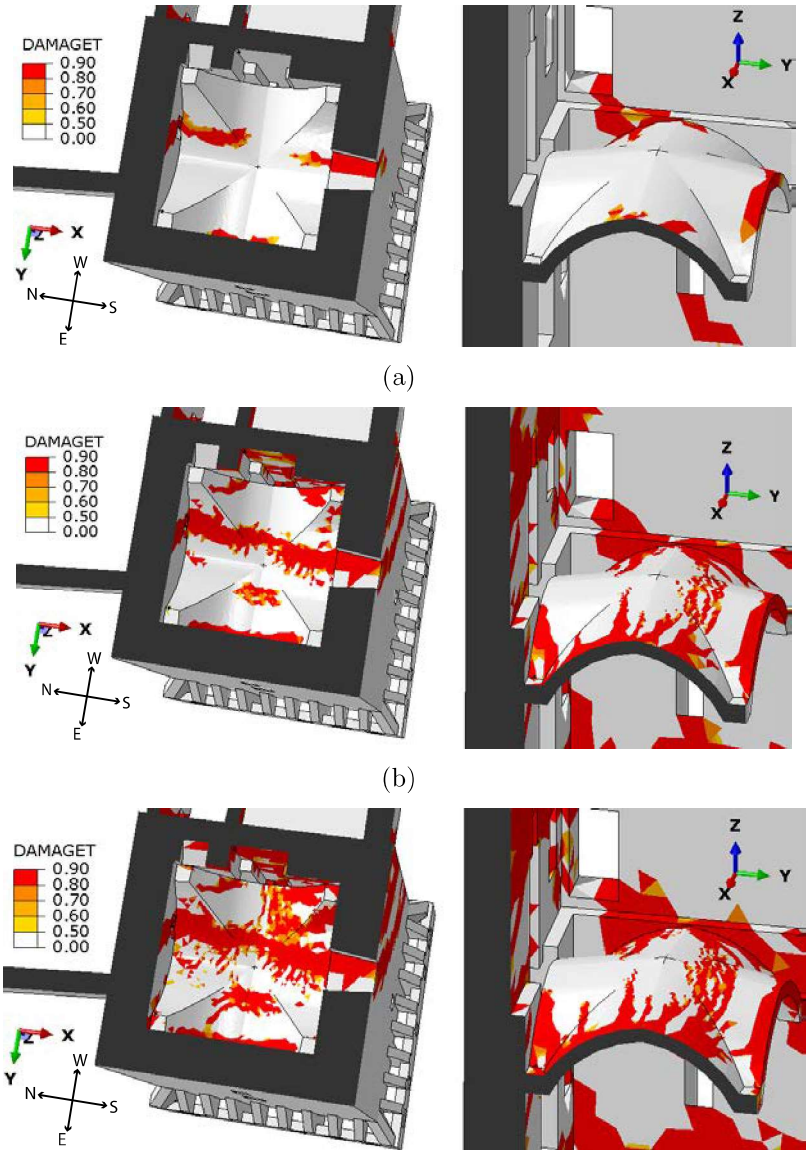

Figure 15: Nonlinear static damage contour plots of the Giulio II Hall's vault, East directed force. Bottom views (left) and section views (right).

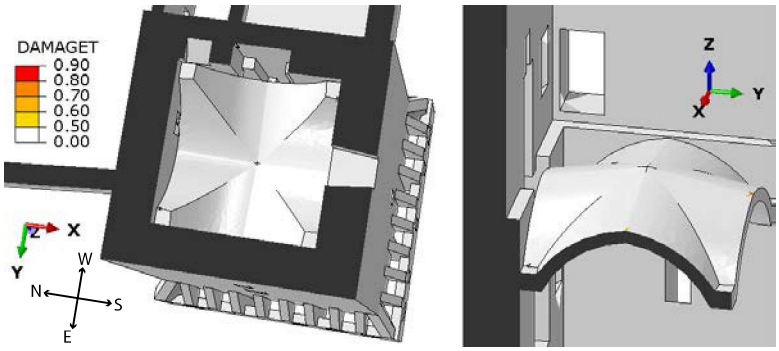

(a)

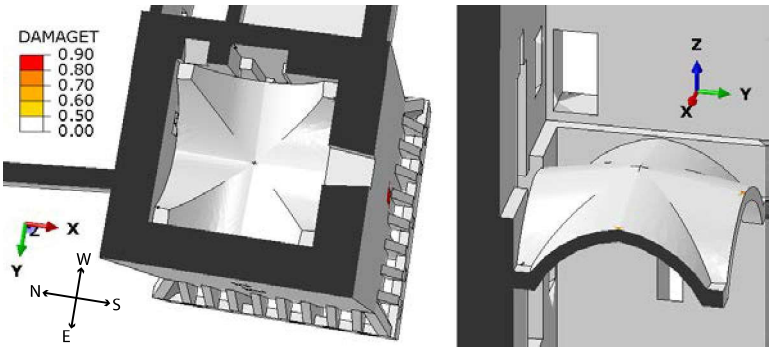

(b)

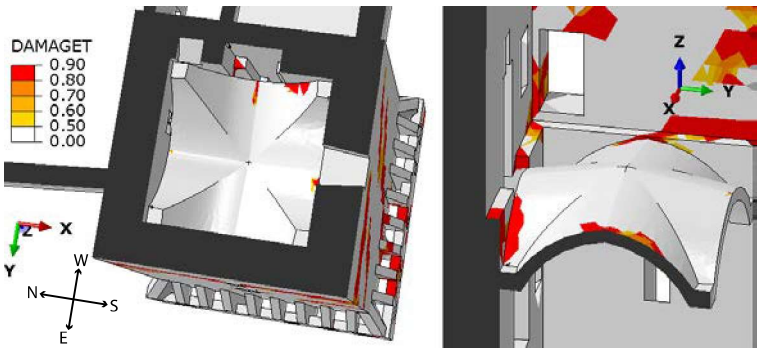

(c)

Figure 16: Nonlinear static damage contour plots of the Giulio II Hall's vault, West directed force. Bottom views (left) and section views (right).

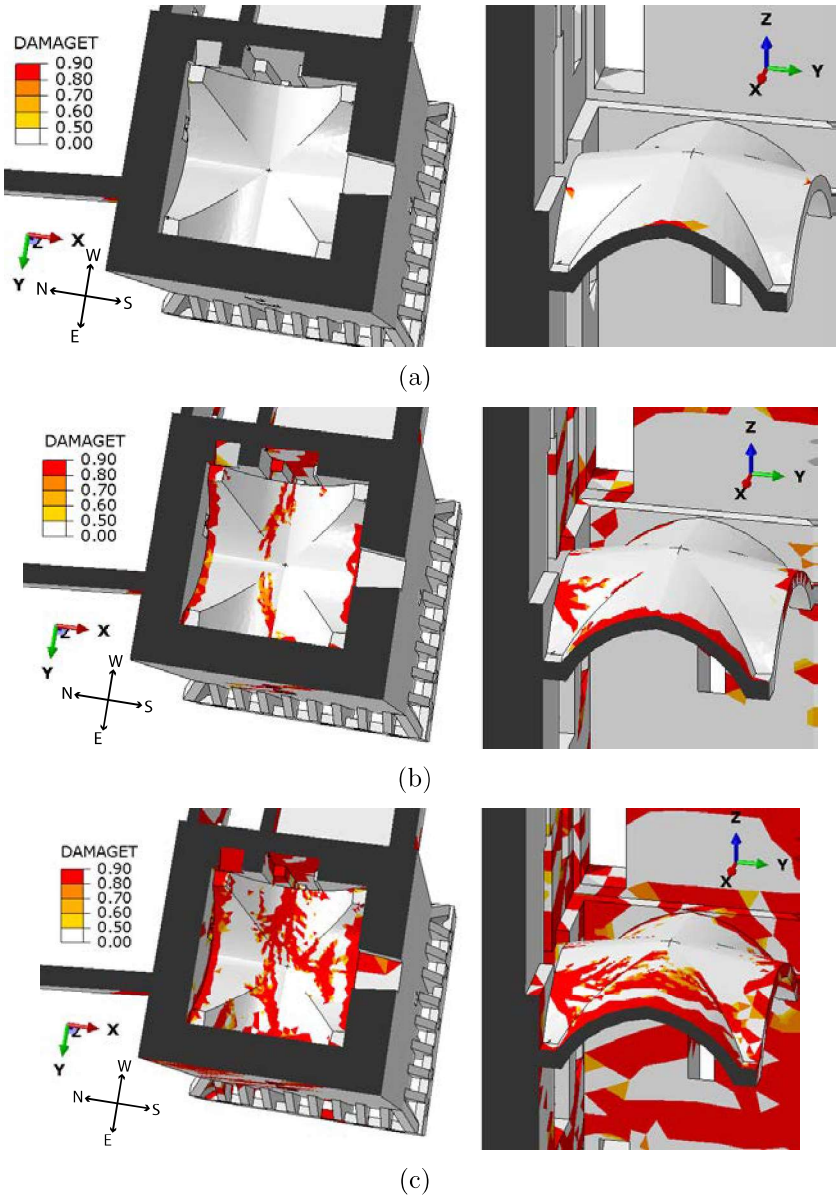

Figure 17: Nonlinear static damage contour plots of the Giulio II Hall's vault, South directed force. Bottom views (left) and section views (right).

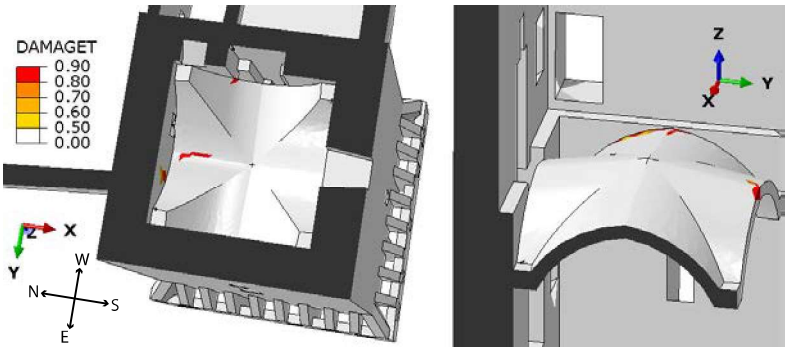

(a)

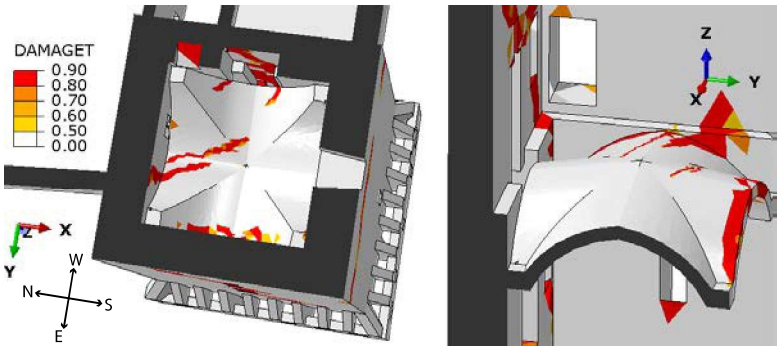

(b)

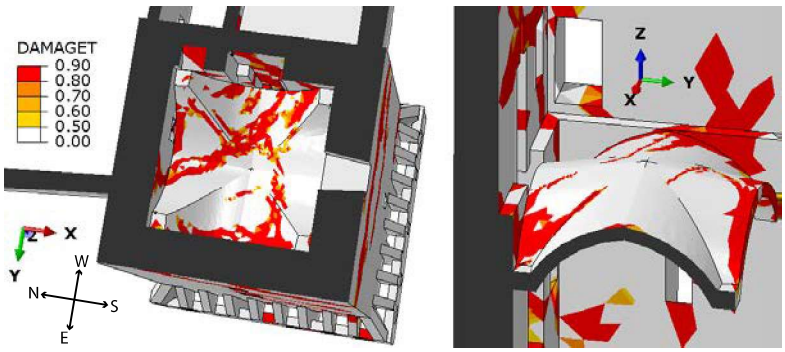

(c)

Figure 18: Nonlinear static damage contour plots of the Giulio II Hall's vault, North directed force. Bottom views (left) and section views (right).

4.2. Nonlinear dynamic analyses

Nonlinear dynamic analyses have been performed using the only actual accelerogram available near to the fortress, recorded on May 29th at the *SAN0* station (installed after the first seismic shock [40, 41]) located at approximately 150 m from the fortress. In particular, 11-seconds simulations have been performed by considering either the horizontal components only or also the vertical component of the accelerogram [42], see Figure 19.

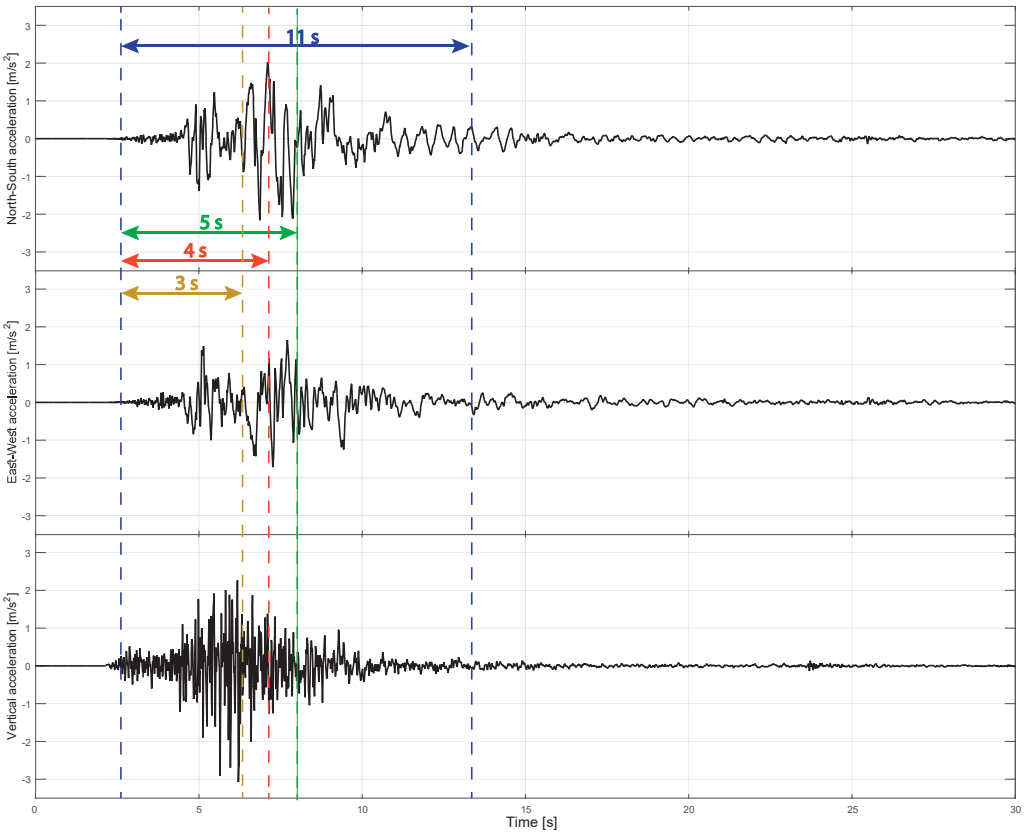

Figure 19: Accelerograms recorded the May 29th 2012 at *SAN0* station.

It is well-known that the dynamic structural response is significantly conditioned by the damping. However, the implementation of damping models for masonry structures in the inelastic regime is still a challenging issue. In dynamic simulations, a Rayleigh damping model has been used, as adopted for masonry structures in [58, 59].

The time-histories of the Giulio II Hall's vault abutments relative displacements are reported in Figure 20 (computed with respect to the point O, see Figure 9(c)). As can be observed in Figure 20, the time-histories of the relative displacements of the vault's abutments of the case without vertical component of the earthquake (Figure 20(a)), are quite similar to the ones of the case with vertical component (Figure 20(b)). However, in the case with vertical component the relative and residual displacements are systematically greater than the case without. By inspecting such time-histories it appears that after the 3rd second of simulation (which corresponds more or less to the peak of the seismic input, see

Figure 19) the vault's abutments tend to significantly distance themselves until the second 5 of the simulation (which corresponds more or less to a significant decrease of the magnitude of the seismic input, see Figure 19), and then they tend to stabilize in residual displacements of several centimeters. Therefore, residual relative displacements have been recorded during the simulations. Table 4 collects such residual displacements of the vault's abutments at the end of the dynamic simulation for both the cases with and without the vertical component of the earthquake. As can be noticed, for both the cases all the sides and diagonals present an increase of length of more than 3 centimeters, exception made for the side AB which presents lower elongations.

Comparing the computed residual relative displacements of Table 4 with the actual one obtained by correlating two different surveys conducted before and after the Emilia earthquake (Table 1), it emerges a quite good agreement between the results even though the computed relative displacements are quite lower than the actual ones. However, it has to be pointed out that the vault has been hit by two main seismic shocks, of which the intensity and the accelerogram of the first one are not available in proximity of the fortress, and no documentation about the crack pattern of the vault between the May 20th and May 29th 2012 is available. Moreover, by also considering the uncertainties in the measures which characterize the 1985's survey, with an order of magnitude of some centimeters, the dynamic simulations results seems reasonably reliable.

The damage contour plots provided by the nonlinear dynamic analyses for subsequent time instants using N-S and E-W components and N-S, E-W and vertical components are depicted in Figures 21 and 22, respectively. In particular, the simulation time instants at 3s, 4s, 5s and 11s are reported since between 3s and 5s the most significant relative displacements occur and the instant 11s represents the end of the simulation.

As far as it is concerned the damage evolution of the case without vertical component (Figure 21), after 3s (Figure 21(a)), cracks in the indrados of the vault begin to develop from the sides parallel to the E-W direction. Then, these cracks evolve and, at 4s (Figure 21(b)), the two limbs tend to link together in the central part. In addition, such limbs join the extremities of the chimney and, at 5s, they are completely connected creating a sort of "rectangle" just in front of the chimney (Figure 21(c)). This finding is in good agreement with the actual crack pattern experienced by the vault, i.e. with the collapse of the portion (a) which presents a pseudo-rectangular shape, see Figure 5(a). Such cracks are also present on the extrados, in a very similar way. Moreover, there is very a good agreement between the crack quasi-perpendicular to the E-W direction, which divides the vault in two parts, with the actual main crack (b) (Figure 4). Finally, the damage pattern at the end of the simulation (11s, see Figure 21(d)) is similar to the one at 5s (Figure 21(c)), as also confirmed by the time-history of the abutments relative displacements of Figure 20 where no substantial changes of displacements are recorded from 5s to 11s.

The damage pattern evolution in the simulation with vertical component (Figure 22) is similar to the one without vertical component (Figure 21). Indeed, also in this case a crack in the intrados of the vault arises (Figure 22(a)), which evolves in a sort of rectangle close to the chimney passing also though the vault in a direction quasi-perpendicular to the East direction. Therefore, also in this case there is a good agreement with the actual crack

pattern. By comparing the damage patterns of the simulations without and with vertical component (Figures 21 and 22, respectively) it appears that the latter is slightly wider than the first.

Finally, it has to be pointed out that, although the failure (a) of Figure 4 seems to be also due to a preexisting stairwell, both the dynamic simulations showed a damage pattern which tends to cut out a pseudo-rectangular portion of the vault in proximity to the chimney hole. Plausibly, this finding could be addressed to the interaction with the chimney hole itself (Figure 9(b)), which represents a weakness of the bearing system. Therefore, in the authors opinion, the likely presence of a preexisting stairwell (and hence of reshuffled material) in such a portion of the vault could have made worse a condition which would already be critical, as arisen from nonlinear dynamic analyses.

Summing up the results, it emerges that the effect of the vertical component of the earthquake is not so significant in studying the seismic response of the vault, even if for strong vertical components (as the studied case), differently for what occurs for overhang structures such as corbels [33]. However, it appears that by considering the vertical component of the earthquake in nonlinear dynamic analyses the obtained results are a bit more conservative.

Table 4: Numerical relative displacements of the vault's abutments at the end of the dynamic simulations.

Without vert. comp.		With vert. comp.	
Rel. displ.	Value	Rel. displ.	Value
ΔOA	3.8 cm	ΔOA	4.9 cm
ΔAB	1.8 cm	ΔAB	0.9 cm
ΔBC	3.1 cm	ΔBC	3.5 cm
ΔCO	5.4 cm	ΔCO	6.6 cm
ΔOB	5.1 cm	ΔOB	5.3 cm
ΔCA	4.3 cm	ΔCA	4.3 cm

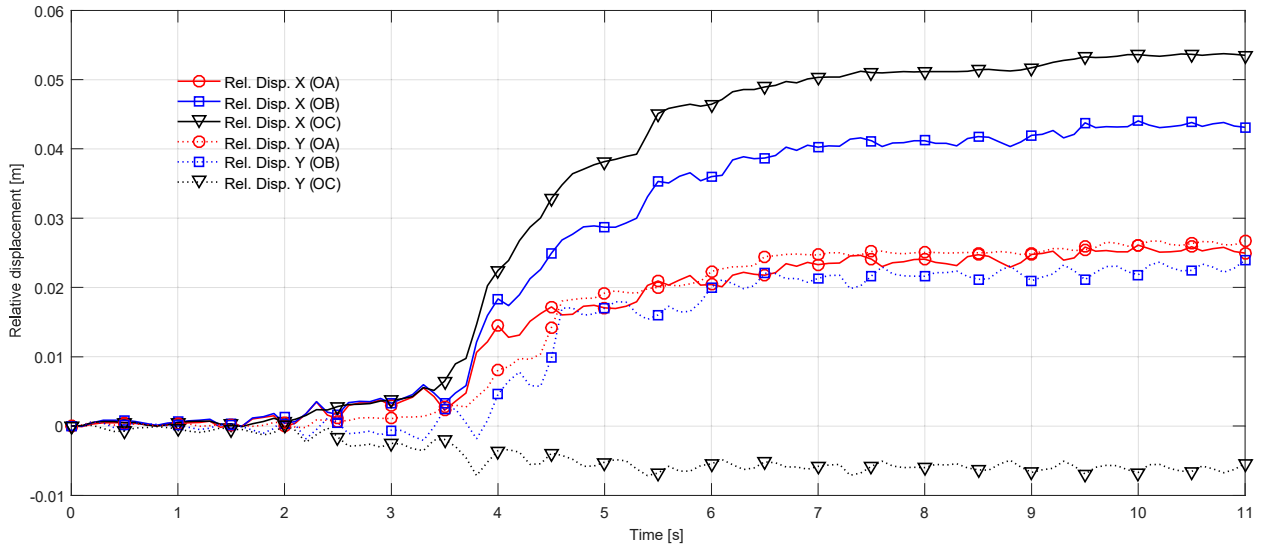

(a)

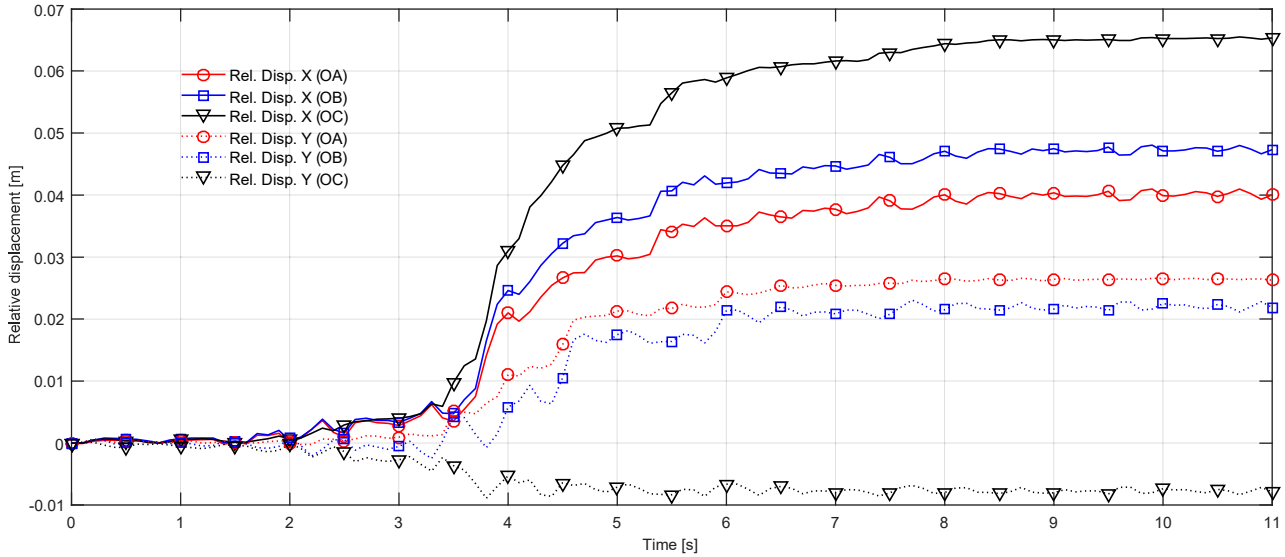

(b)

Figure 20: Vault's abutments relative displacements time-histories measured in nonlinear dynamic analyses: (a) without and (b) with vertical component of the earthquake.

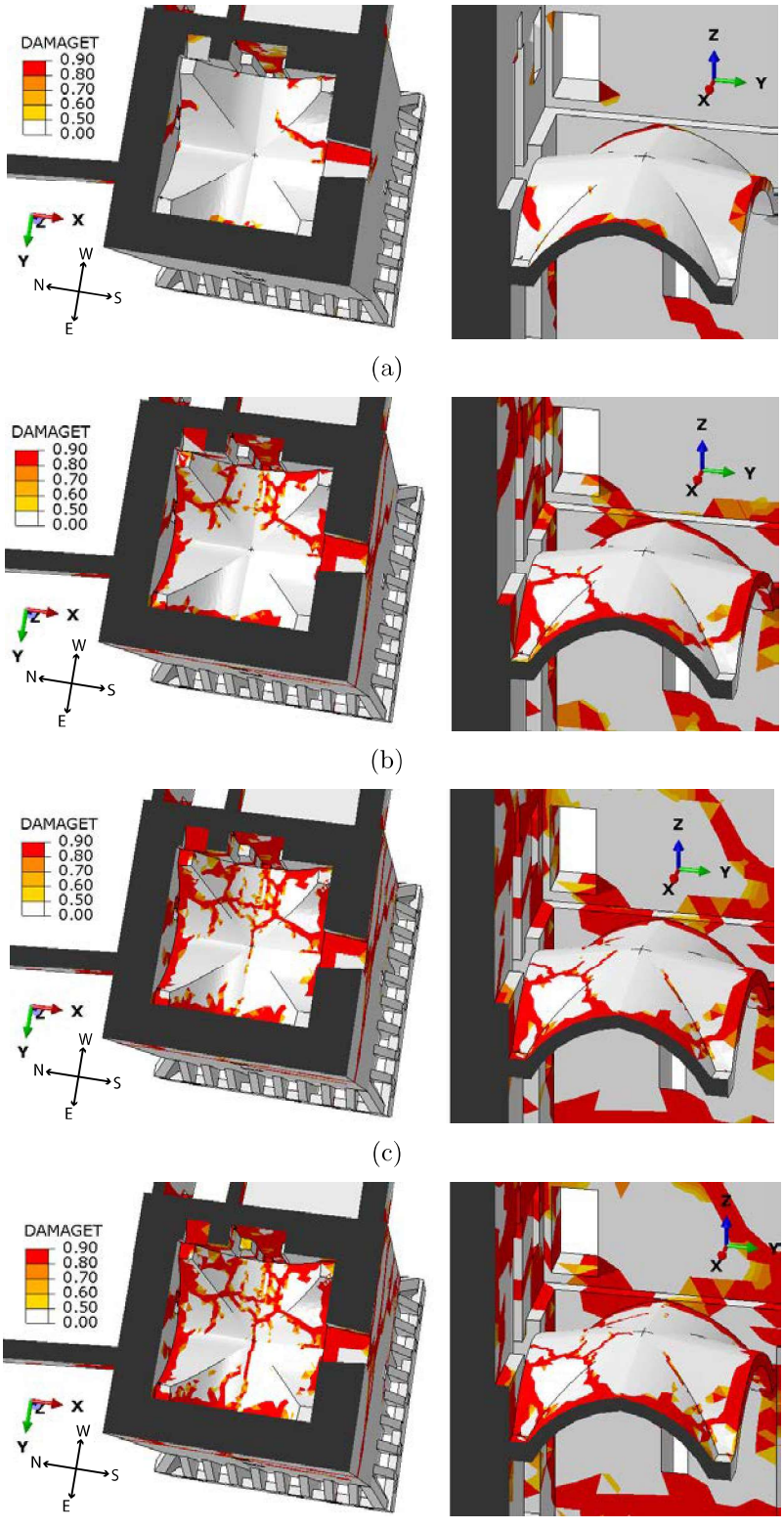

Figure 21: Nonlinear dynamic damage contour plots of the Giulio II Hall's vault, simulation without vertical component. Bottom views (left) and section views (right) at instants (a) 3s, (b) 4s, (c) 5s and (d) 11s.

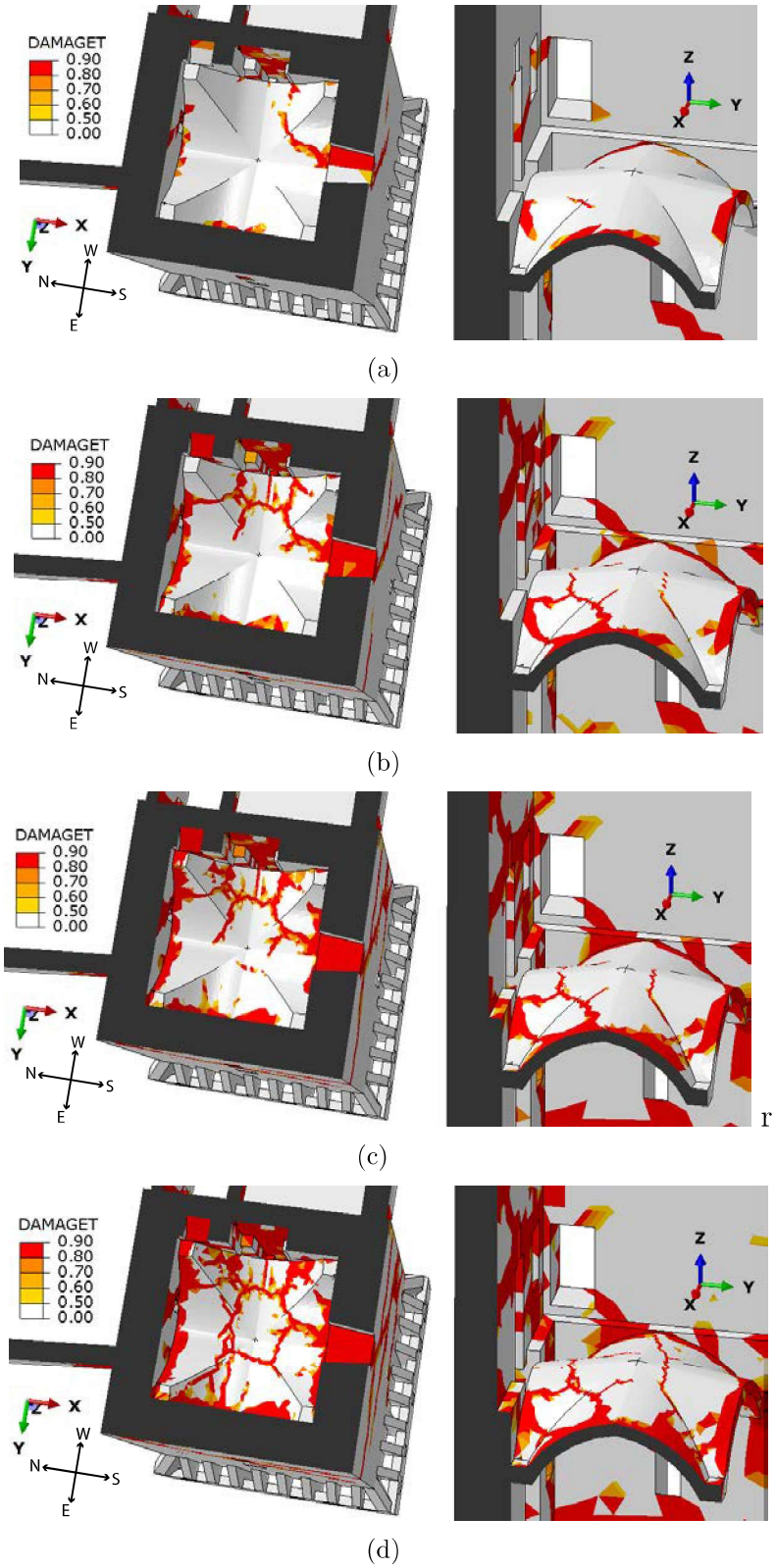

Figure 22: Nonlinear dynamic damage contour plots of the Giulio II Hall's vault, simulation with vertical component. Bottom views (left) and section views (right) at instants (a) 3s, (b) 4s, (c) 5s and (d) 11s.

5. Concluding remarks

In this paper, an investigation of the capabilities and limitations of current computational tools to analyze the seismic-induced damage in a masonry vaulted structure has been presented. The case under study was the Giulio II vault, located within the main tower of the San Felice sul Panaro fortress (Italy) which has been severely damaged by the 2012 Emilia earthquake. Attention has been focused on the interaction between the vault and its bearing tower. The developed finite element model included the 3D geometry of the vault within the geometry of the tower, based on a before-quake survey.

Nonlinear static and dynamic analyses have been carried out by using a damage-plasticity constitutive law for masonry. The results have been compared to the vault actual crack pattern as well as to its actual-deformed geometry based on a post-quake laser scanner survey. On the one hand, concerning the damage contour plots, it emerged that both those of nonlinear static and dynamic analyses were in good agreement with the main failures experienced by the vault. Conversely, coarse findings has been obtained with respect to smaller cracks, for which the masonry arrangement, not contemplated in the implemented damage model, plays a more considerable role than for main failures. On the other hand, lower accuracy has been obtained in the prediction of the relative displacements of the vault's abutments. Although nonlinear static analyses are a conventional procedure for the safety evaluation of structures, they are qualitatively able to investigate the main weaknesses of the vault, helping the interpretation of (more comprehensive) dynamic analyses results. Therefore, both nonlinear static and dynamic FE analyses appear to be useful tools for the seismic-induced damage investigation of masonry vaults, and for assessing the main weaknesses of such structures.

Finally, it emerged that the seismic behavior of the tower (and also the presence of adjacent buildings) strongly influence the damage of the vault. Thereby, in order to investigate the seismic-induced damage of a masonry vault, the numerical modeling of the vault should be considered within the model of the bearing structure (walls, columns, etc.), given their mutual remarkable interaction.

Acknowledgments

The authors would like to thank ABACUS (`http://www.arcoabacus.it`), the municipality of San Felice sul Panaro (MO) and Eng. Stefano Magagnini. Financial support by the Italian Ministry of Education, Universities and Research MIUR is gratefully acknowledged (PRIN2015 "Advanced mechanical modeling of new materials and structures for the solution of 2020 Horizon challenges" prot. 2015JW9NJT_018).

References

[1] Preciado, A. Seismic vulnerability and failure modes simulation of ancient masonry towers by validated virtual finite element models. Engineering Failure Analysis 2015, 57, 72-87.

[2] Clementi, F.; Gazzani, V.; Poiani, M.; Lenci, S. Assessment of seismic behaviour of heritage masonry buildings using numerical modelling. Journal of Building Engineering 2016, 8, 2947. doi:10.1016/j.jobe.2016.09.005

[3] Cattari, S.; Resemini, S.; Lagomarsino, S.. Modelling of vaults as equivalent diaphragms in 3D seismic analysis of masonry buildings. In Proceedings of 6th international conference on structural analysis of historic construction, 2008, Bath, UK.

[4] Çaktı, E.; Saygili, O.; Dar, E.; Ercan T. Seismic behavior of the Edirnerkapi Mihrimah Sultan Mosque in Istanbul. In Proceedings of the 6th ECCOMAS Thematic Conference on Computational Methods in Structural Dynamics and Earthquake Engineering, (Rhodes Island, Greece), 2017.

[5] Croci G. The Basilica of St. Francis of Assisi after the September 1997 Earthquake. Structural Engineering International 1998, 8(1), 56-58. doi:10.2749/101686698780489667

[6] S. Huerta. The analysis of masonry architecture: A historical approach. Architectural Science Review 2008, 51(4), 297328.

[7] M. Como. Statics of historic masonry constructions. Springer-Verlag, Berlin, Germany, 2013.

[8] Heyman, J. Equilibrium of shell structures, Clarendon Press, Oxford, 1977.

[9] Heyman, J. The stone skeleton: Structural engineering of masonry architecture. Cambridge University Press, 1995.

[10] Chiarugi, A.; Fanelli, A.; Giuseppetti, G. Diagnosis and strengthening of the Brunelleschi Dome. In Proceedings of IABSE Symposium, 1993, IABSE, Zurich, Switzerland, 441-448.

[11] Tralli, A.; Alessandri, C.; Milani, G. Computational Methods for Masonry Vaults: A Review of Recent Results. The Open Civil Engineering Journal 2014, 8(1), 272-287.

[12] Block, P.; Lachauer, L. Three-Dimensional (3D) Equilibrium Analysis of Gothic Masonry Vaults. International Journal of Architectural Heritage 2013, 8(3), 312-335. doi:10.1080/15583058.2013.826301

[13] Andreu, A.; Gil, L.; Roca, P. Computational Analysis of Masonry Structures with a Funicular Model. Journal of Engineering Mechanics 2007, 133(4), 473-480. doi:10.1061/(asce)0733-9399(2007)133:4(473)

[14] Fraternali, F.; Angelillo, M.; Fortunato, A. A lumped stress method for plane elastic problems and the discrete-continuum approximation. International Journal of Solids and Structures 2002, 39(25), 6211-6240. doi:10.1016/s0020-7683(02)00472-9

[15] D'Ayala, D. F.; Tomasoni, E. Three-Dimensional Analysis of Masonry Vaults Using Limit State Analysis with Finite Friction. International Journal of Architectural Heritage 2011, 5(2), 140-171. doi:10.1080/15583050903367595

[16] Marmo, F.; Rosati, L. Reformulation and extension of the thrust network analysis. Computers & Structures 2017, 182, 104-118. doi:10.1016/j.compstruc.2016.11.016

[17] Carini, A.; Genna, F. Stability and strength of old masonry vaults under compressive longitudinal loads: Engineering analyses of a case study. Engineering Structures 2012, 40, 218-229. doi:10.1016/j.engstruct.2012.02.028

[18] Theodossopoulos, D.; Sinha, B. P.; Usmani, A. S.; Macdonald, A. J. Assessment of the Structural Response of Masonry Cross Vaults. Strain 2002, 38(3), 119127. doi:10.1046/j.0039-2103.2002.00021.x

[19] Creazza, G.; Matteazzi, R.; Saetta, A.; Vitaliani, R. Analyses of Masonry Vaults: A Macro Approach based on Three-Dimensional Damage Model. Journal of Structural Engineering 2002, 128(5), 646-654. doi:10.1061/(asce)0733-9445(2002)128:5(646)

[20] Milani, E.; Milani, G.; Tralli, A. Limit analysis of masonry vaults by means of curved shell finite elements and homogenization. International Journal of Solids and Structures 2008, 45(20), 5258-5288. doi:10.1016/j.ijsolstr.2008.05.019

[21] Milani G.; Valente M.; Alessandri C. The narthex of the Church of the Nativity in Bethlehem: a non-linear finite element approach to predict the structural damage. Computers & Structures 2017. In press. Doi: 10.1016/j.compstruc.2017.03.010

[22] Milani G.; Valente M.; Alessandri C. Advanced numerical insight into the structural damage of masonry vaults under seismic excitation: two valuable case-studies. International Journal of Masonry Research and Innovation. In press (forthcoming Vol 2 Issue 2 pages:xx-yy)

[23] P.B. Lourenço, Computational strategies for masonry structures, Ph.D. Thesis, Delft University Press, Delft (The Netherlands), 1996.

[24] Girardi, M.; Padovani, C.; Pellegrini, D. The NOSA-ITACA code for the safety assessment of ancient constructions: A case study in Livorno. Advances in Engineering Software 2015, 89, 64-76.

552 doi:10.1016/j.advengsoft.2015.04.002
553 [25] Caliò, I.; Cannizzaro, F.; Marletta, M. A Discrete Element for Modeling Masonry Vaults. Advanced
554 Materials Research 2010, 133-134, 447-452. doi:10.4028/www.scientific.net/amr.133-134.447
555 [26] Milani, G.; Rossi, M.; Calderini, C.; Lagomarsino, S. Tilting plane tests on a small-scale masonry cross
556 vault: Experimental results and numerical simulations through a heterogeneous approach. Engineering
557 Structures 2016, 123, 300-312. doi:10.1016/j.engstruct.2016.05.017
558 [27] Sarhosis, V.; Bagi, K.; Lemos, J.; Milani, G. Computational Modeling of Masonry Structures Using
559 the Discrete Element Method. Hershey, PA: IGI Global, 2016. doi:10.4018/978-1-5225-0231-9
560 [28] Castellazzi, G.; DAltri, A.M.; Bitelli, G.; Selvaggi, I.; Lambertini, A. From Laser Scanning to Finite
561 Element Analysis of Complex Buildings by Using a Semi-Automatic Procedure. Sensors 2015, 15(8),
562 18360-18380. doi:10.3390/s150818360
563 [29] Castellazzi, G.; DAltri, A. M.; de Miranda, S.; Ubertini, F. An innovative numerical modeling strategy
564 for the structural analysis of historical monumental buildings. Engineering Structures 2017, 132, 229-
565 248. doi:10.1016/j.engstruct.2016.11.032
566 [30] Castellazzi, G.; D'Altri, A.M.; de Miranda, S.; Ubertini, F.; Bitelli, G.; Lambertini, A.; Selvaggi, I.;
567 Tralli, A. A mesh generation method for historical monumental buildings: an innovative approach.
568 ECCOMAS Congress 2016 - Proceedings of the 7th European Congress on Computational Methods
569 in Applied Sciences and Engineering, 2016, 1, 409-416.
570 [31] Degli Abbati, S.; D'Altri, A.M.; Ottonelli, D.; Castellazzi, G.; Cattari, S.; de Miranda, S.; Lago-
571 marsino, S. Seismic assessment of complex assets through nonlinear static analyses: the fortress in San
572 Felice sul Panaro hit by the 2012 earthquake in Italy. In Proceedings of the 6th ECCOMAS Thematic
573 Conference on Computational Methods in Structural Dynamics and Earthquake Engineering, (Rhodes
574 Island, Greece), 2017.
575 [32] Forghieri, M.; Bassoli, E.; Vincenzi, L. Dynamic behaviour of the San Felice sul Panaro fortress: Ex-
576 perimental tests and model updating. In Proceedings of the 6th ECCOMAS Thematic Conference
577 on Computational Methods in Structural Dynamics and Earthquake Engineering, (Rhodes Island,
578 Greece), 2017.
579 [33] Castellazzi, G.; D'Altri, A.M.; de Miranda, S.; Magagnini, S.; Tralli, A. On the seismic behavior of
580 the main tower of San Felice sul Panaro (Italy) fortress. AIP Conference Proceedings 2016, 1790(1),
581 130009. doi: 10.1063/1.4968727
582 [34] Castellazzi, G.; D'Altri, A.M.; de Miranda, S.; Chiozzi, A.; Tralli, A. Numerical insights on the seismic
583 behavior of a non-isolated historical masonry tower. (Submitted).
584 [35] Lagomarsino, S.; Cattari, S. PERPETUATE guidelines for seismic performance-based assessment of
585 cultural heritage masonry structures. Bulletin of Earthquake Engineering 2015, 13(1), 13-47.
586 [36] Parisi, F.; Augenti, N. Earthquake damages to cultural heritage constructions and simplified assess-
587 ment of artworks. Engineering Failure Analysis 2013, 34, 735-760. doi:10.1016/j.engfailanal.2013.01.005
588 [37] Milani, G. Lesson learned after the Emilia-Romagna, Italy, 2029 May 2012 earthquakes: A
589 limit analysis insight on three masonry churches. Engineering Failure Analysis 2013, 34, 761-778.
590 doi:10.1016/j.engfailanal.2013.01.001
591 [38] Milani, G.; Valente, M. Comparative pushover and limit analyses on seven masonry churches dam-
592 aged by the 2012 Emilia-Romagna (Italy) seismic events: Possibilities of non-linear finite elements
593 compared with pre-assigned failure mechanisms. Engineering Failure Analysis 2015, 47, 129-161.
594 doi:10.1016/j.engfailanal.2014.09.016
595 [39] Milani, G.; Valente, M. Failure analysis of seven masonry churches severely damaged during the 2012
596 Emilia-Romagna (Italy) earthquake: Non-linear dynamic analyses vs conventional static approaches.
597 Engineering Failure Analysis 2015, 54, 13-56. doi:10.1016/j.engfailanal.2015.03.016
598 [40] Dolce, M.; Nicoletti, N.; Ammirati, A.; Bianconi, R.; Filippi, L.; Gorini, A.; Marcucci, S.; Palma,
599 F.; Zambonelli, E.; Lavecchia, G.; de Nardis, R.; Brozzetti, F.; Boncio, P.; Cirillo, D.; Romano, A.;
600 Costa, G.; Gallo, A.; Tiberi, L.; Zoppè, G.; Suhadolc, P.; Ponziani, F.; Formica, A. The Emilia thrust
601 earthquake of 20 May 2012 (Northern Italy): strong motion and geological observations–report I, 2012.
602 www.protezionecivile.gov.it/resources/cms/documents/Report_DPC_1_Emilia_EQSd.pdf

[41] Dolce, M.; Nicoletti, N.; Ammirati, A.; Bianconi, R.; Filippi, L.; Gorini, A.; Marcucci, S.; Palma, F.; Zambonelli, E.; Lavecchia, G.; de Nardis, R.; Brozzetti, F.; Boncio, P.; Cirillo, D.; Romano, A.; Costa, G.; Gallo, A.; Tiberi, L.; Zoppè, G.; Suhadolc, P.; Ponziani, F.; Formica, A. The Ferrara arc thrust earthquakes of May-June 2012 (Northern Italy): strong-motion and geological observations–report II, 2012. www.protezionecivile.gov.it/resources/cms/documents/report_DPC_2_Emilia_EQSBis.pdf

[42] Luzi, L.; Hailemikael, S.; Bindi, D.; Pacor, F.; Mele, F. ITACA (ITalian ACcelerometric Archive): A web portal for the dissemination of Italian strong motion data, Seismological Research Letters 2008, 79, 716-722.

[43] Cattari, S.; Degli Abbati, S.; Ferretti, D.; Lagomarsino, S.; Ottonelli, D.; Tralli, A. Damage assessment of fortresses after the 2012 Emilia earthquake (Italy). Bulletin of Earthquake Engineering 2014, 12, 2333-2365.

[44] Alexander, K. D.; Mark, R.; Abel, J. F. The Structural Behavior of Medieval Ribbed Vaulting. Journal of the Society of Architectural Historians 1977, 36(4), 241-251.

[45] Lengyel, G.; Bagi, K. Numerical analysis of the mechanical role of the ribs in groin vaults. Computers & Structures 2015, 158, 42-60.

[46] Page, A.W. The biaxial compressive strength of brick masonry. In Proceeding of the Institution of Civil Engineers 1981, Part 2, 71, 893-906.

[47] Luciano, R.; Sacco, E. Homogenization technique and damage model for old masonry material. International Journal of Solids and Structures 1997, 34(24), 3191-3208.

[48] Abaqus®. Theory manual, version 6.14; 2014.

[49] Lubliner, J.; Oliver, J.; Oller, S.; Oñate, E. A plastic-damage model for concrete. International Journal of Solids and Structures 1989, 25(3), 299-326. doi:10.1016/0020-7683(89)90050-4

[50] Lee, J.; Fenves, G. L. Plastic-Damage Model for Cyclic Loading of Concrete Structures. Journal of Engineering Mechanics 1998, 124(8), 892-900. doi:10.1061/(asce)0733-9399(1998)124:8(892)

[51] Van Der Pluijm. Shear Behaviour of bed joints. In: Abrams DP, editor. Proceedings of 6th North American masonry conference, Philadelphia, USA, 6-9 June, 1993, 125-136.

[52] Valente, M.; Milani, G. Seismic assessment of historical masonry towers by means of simplified approaches and standard FEM. *Construction and Building Materials* 2016, *108*, 74-104.

[53] Acito, M.; Chesi, C.; Milani, G.; Torri, S. Collapse analysis of the Clock and Fortified towers of Finale Emilia, Italy, after the 2012 Emilia Romagna seismic sequence: Lesson learned and reconstruction hypotheses. Construction and Building Materials 2016, 115 , 193-213.

[54] DM 14/01/2008. Nuove norme tecniche per le costruzioni. Ministero delle Infrastrutture (GU n.29 04/02/2008), Rome, Italy [New technical norms on constructions].

[55] Circolare n 617 del 2 Febbraio 2009. Istruzioni per l'applicazione delle nuove norme tecniche per le costruzioni di cui al decreto ministeriale 14 Gennaio 2008 [Instructions for the application of the new technical norms on constructions].

[56] DPCM 9/2/2011. Linee guida per la valutazione e la riduzione del rischio sismico del patrimonio culturale con riferimento alle Norme tecniche delle costruzioni di cui al decreto del Ministero delle Infrastrutture e dei trasporti del 14 gennaio 2008 [Italian guidelines for the evaluation and reduction of the seismic risk of cultural heritage, with reference to the Italian norm of constructions].

[57] Borri, A.; Cangi, G.; De Maria, A. Caratterizzazione meccanica delle murature (anche alla luce del recente sisma in Emilia) e interpretazione delle prove sperimentali a taglio. In Proceedings of ANIDIS Congress, Associazione Nazionale Italiana Di Ingegneria Sismica, 2013, Padua, Italy [Mechanical characterization of masonry (considering also the recent Emilia earthquake) and interpretation of shear experimental tests].

[58] Pineda, P. Collapse and upgrading mechanisms associated to the structural materials of a deteriorated masonry tower. Nonlinear assessment under different damage and loading levels. Engineering Failure Analysis 2016, 63, 72-93.

[59] Chiozzi, A.; Simoni, M.; Tralli, A. Base isolation of heavy non-structural monolithic objects at the top of a masonry monumental construction. Materials and Structures 2015, 49(6), 2113-2130.